

# Dimension-independent Markov chain Monte Carlo on the sphere

H. C. Lie<sup>1</sup>    D. Rudolf<sup>2</sup>    B. Sprungk<sup>3</sup>    T. J. Sullivan<sup>4,5</sup>

February 28, 2022

**Abstract.** We consider Bayesian analysis on high-dimensional spheres with angular central Gaussian priors. These priors model antipodally-symmetric directional data, are easily defined in Hilbert spaces and occur, for instance, in Bayesian binary classification and level set inversion. In this paper we derive efficient Markov chain Monte Carlo methods for approximate sampling of posteriors with respect to these priors. Our approaches rely on lifting the sampling problem to the ambient Hilbert space and exploit existing dimension-independent samplers in linear spaces. By a push-forward Markov kernel construction we then obtain Markov chains on the sphere, which inherit reversibility and spectral gap properties from samplers in linear spaces. Moreover, our proposed algorithms show dimension-independent efficiency in numerical experiments.

**Keywords.** Markov chain Monte Carlo • dimension independence • directional statistics • level set inversion • high-dimensional manifolds

**2020 Mathematics Subject Classification.** 46T12 • 58C35 • 60J22 • 62H11 • 65C40

## 1. Introduction

The Markov chain Monte Carlo (MCMC) method is a standard tool for computational probability and recent years have seen increasing interest in *dimension-independent* MCMC schemes, i.e. those whose statistical efficiency and mixing rates do not degenerate to zero as the dimension of the sample space tends to infinity. We mention here the preconditioned Crank–Nicolson (pCN) scheme of [Cotter et al. \(2013\)](#) — see also ([Neal, 1999](#), Equation (15)) and ([Beskos et al., 2008](#)) — as well as the elliptical slice sampler (ESS) of [Murray et al. \(2010\)](#), both of which rely on a Gaussian reference/prior measure. Recently, the pCN scheme has been combined with geometric MCMC methods ([Beskos et al., 2017](#); [Rudolf and Sprungk, 2018](#)) and extended to classes of non-Gaussian priors ([Chen et al., 2018](#)), and for the ESS geometric ergodicity was shown by [Natarovskii et al. \(2021a\)](#).

In this work, we study whether these dimension-independent sampling schemes could also be modified for Bayesian analysis on high-dimensional manifolds. As a starting point we focus on

<sup>1</sup>Institut für Mathematik, Universität Potsdam, Karl-Liebknecht-Straße 24–25, 14476 Potsdam OT Golm, Germany ([hanlie@uni-potsdam.de](mailto:hanlie@uni-potsdam.de))

<sup>2</sup>Universität Passau, Innstraße 33, 94032 Passau, Germany ([daniel.rudolf@uni-passau.de](mailto:daniel.rudolf@uni-passau.de))

<sup>3</sup>Technische Universität Bergakademie Freiberg, 09596 Freiberg, Germany ([bjoern.sprungk@math.tu-freiberg.de](mailto:bjoern.sprungk@math.tu-freiberg.de))

<sup>4</sup>Mathematics Institute and School of Engineering, University of Warwick, Coventry, CV4 7AL, United Kingdom ([t.j.sullivan@warwick.ac.uk](mailto:t.j.sullivan@warwick.ac.uk))

<sup>5</sup>Alan Turing Institute, 96 Euston Road, London, NW1 2DB, United Kingdom

Bayesian inference on high-dimensional spheres (Watson, 1983). However, several of our results are valid for general manifolds. Our choice of the sphere is further motivated by particular inverse problems on function spaces such as level set inversion — more precisely, *binary classification* — where one is essentially interested only in recovering the pointwise *sign* of a function  $u: D \rightarrow \mathbb{R}$  on some domain  $D$ . Thus,  $u$  and  $\alpha u$  for  $\alpha > 0$  yield equivalent classifications and, hence, it is natural to consider the inverse problem just on some unit sphere of functions.

Previous works on Markov chain Monte Carlo methods on manifolds — such as those of Brubaker et al. (2012), Byrne and Girolami (2013), Diaconis et al. (2013), Mangoubi and Smith (2018), and Zappa et al. (2018) — derive algorithms which are based on the Hausdorff or surface measure, as reference measure. However, despite their use of geometric structure, the performance of such methods typically still degrade as the dimension of the sample space increases to infinity — one reason being the degeneration of the target density with respect to the Hausdorff measure.

### 1.1. Contribution

In this paper, we aim to construct dimension-independent MCMC methods in order to sample efficiently from target measures given on high-dimensional spheres. We identified the angular central Gaussian (ACG) distribution as a suitable reference measure for this purpose. The ACG models antipodal symmetric directional data and is an alternative to the Bingham distribution (Tyler, 1987). ACG distributions and their mixtures have been applied in finite-dimensional directional-statistical problems, such as geomagnetism (Tyler, 1987, Section 8), imaging in neuroscience (Tabelow et al., 2012), and materials science (Franke et al., 2016, Section 4). ACG distributions have been generalised to the projected normal distribution which allow the initial Gaussian distribution to have nonzero mean (Wang and Gelfand, 2013).

The ACG distribution is defined as the radial projection onto the sphere of a centred Gaussian measure on the ambient Hilbert space and thus yields a well-defined reference measure even in infinite dimensions. Moreover, the ACG distribution can be applied in an acceptance-rejection method for sampling from several families of distributions on spheres and similar manifolds (Kent et al., 2018). Thus, we anticipate that our proposed methods could potentially also be exploited for dimension-independent MCMC for posteriors with other priors, e.g. Bingham priors (Dryden, 2005). However, we leave this question for future research, and focus on posteriors given with respect to the ACG prior in this paper.

The particular structure of the ACG prior allows us to lift the sampling problem to the ambient Hilbert space. Thus, we can exploit existing dimension-independent MCMC algorithms on linear spaces, e.g. the pCN algorithm mentioned earlier. In order to obtain Markov chains on the sphere, we use the methodology of *push-forward Markov kernels* (Rudolf and Sprungk, 2022). This approach then yields specific MCMC algorithms that first draw from a suitable distribution a point on the ray defined by the current position on the sphere, and then take a step using a dimension-independent transition kernel. The resulting state is finally “reprojected” to the sphere. In summary, our contributions are as follows:

- (1) We propose two easily implementable MCMC algorithms that generate reversible Markov chains on high-dimensional spheres, where the chains have as their invariant distribution a given posterior with respect to an ACG prior;
- (2) We prove uniform ergodicity of the suggested Markov chains in finite-dimensional settings;
- (3) We provide theoretical arguments for as well as numerical illustrations of dimension independent statistical efficiency of the proposed algorithms.

Moreover, our numerical experiments show that some other existing MCMC methods for sampling on manifolds — see Section 1.3 for an overview — exhibit decreasing statistical efficiency

as the state space dimension increases. Thus, we provide a first contribution to dimension-independent MCMC on manifolds, and thereby demonstrate the feasibility of efficient Bayesian analysis on high-dimensional spheres.

## 1.2. Outline

The remainder of this paper is structured as follows. [Section 1.3](#) overviews some related work in this area. [Section 2](#) sets out our basic notation, recalls some key facts about Gaussian measures, and precisely defines the ACG measure on the sphere. [Section 3](#) sets out definitions and basic properties related to MCMC, in particular the Metropolis–Hastings (MH) and slice sampling paradigms. Then, in [Section 4](#), we make our main theoretical contributions by developing a general framework for obtaining dimension-independent MCMC methods on manifolds and, particularly, deriving and analysing two sampling methods on the sphere. These methods are subjected to numerical tests, in the context of binary classification, in [Section 5](#). Some closing remarks are given in [Section 6](#), and technical auxiliary results are given in [Appendix A](#).

## 1.3. Overview of related work

Classical references that treat statistical inference on the sphere include those of [Watson \(1983\)](#), who focuses exclusively on spheres in finite-dimensional Euclidean spaces, and [Mardia and Jupp \(2000\)](#), who focus on circular data but also treat spheres, Stiefel and Grassmann manifolds, and general manifolds. Special manifolds such as the Stiefel and Grassmann manifolds have also been studied by [Chikuse \(2003\)](#). A recent treatment that focuses on modern developments in directional statistics is given by [Ley and Verdebout \(2017\)](#). [Srivastava and Jermyn \(2009\)](#) consider the infinite-dimensional unit sphere of diffeomorphisms in the context of computer vision, and then apply a Bayesian method for shape identification. However, none of the cited works treat MCMC sampling methods or Bayesian inference on high-dimensional manifolds.

Regarding sampling on embedded manifolds, Hamiltonian Monte Carlo methods are considered by [Brubaker et al. \(2012\)](#) and [Byrne and Girolami \(2013\)](#), for instance, and [Diaconis et al. \(2013\)](#) propose a Gibbs sampler. Moreover, [Mangoubi and Smith \(2018\)](#) study the so-called “geodesic walk” algorithm and establish Wasserstein contraction, under the assumption that the manifold has bounded, positive curvature. The geodesic walk algorithm of [Mangoubi and Smith \(2018\)](#) chooses a random element uniformly from the unit sphere in the tangent space and moves a fixed time or step size along the corresponding geodesic. This could be used as a proposal in a MH algorithm. Similarly, [Zappa et al. \(2018\)](#) developed a MH algorithm on manifolds where the proposed point is generated by a normally distributed tangential move into the ambient Euclidean space which is then suitably projected back to the manifold. We will compare our algorithms particularly to the one by [Zappa et al. \(2018\)](#) as well as to the geodesic walk algorithm of [Mangoubi and Smith \(2018\)](#). For the specific problem of designing MCMC samplers on the sphere, [Lan et al. \(2014\)](#) considered Hamiltonian Monte Carlo for distributions that undergo several transformations in order to be defined on the unit sphere. Their approach has been used by, e.g. [Holbrook et al. \(2020\)](#) to perform Bayesian nonparametric density estimation based on the Bingham distribution as the prior.

## 2. Preliminaries and notation

Throughout,  $(\Omega, \mathcal{A}, \mathbb{P})$  will be a fixed probability space, which we assume to be rich enough to serve as a common domain of definition for all random variables under consideration.

Given a topological space  $\mathbb{X}$ ,  $\mathcal{B}(\mathbb{X})$  will denote the Borel  $\sigma$ -algebra on  $\mathbb{X}$ , and  $\mathcal{P}(\mathbb{X})$  will denote the space of probability measures on  $(\mathbb{X}, \mathcal{B}(\mathbb{X}))$ . Given another topological space  $\mathbb{Y}$ ,  $T_{\#}\mu \in \mathcal{P}(\mathbb{Y})$  will denote the *push-forward* or *image measure* of  $\mu \in \mathcal{P}(\mathbb{X})$  under a measurable map  $T: \mathbb{X} \rightarrow \mathbb{Y}$ , i.e.

$$(T_{\#}\mu)(E) := \mu(T^{-1}(E)) \equiv \mu(\{x \in \mathbb{X} \mid T(x) \in E\}) \quad \text{for each } E \in \mathcal{B}(\mathbb{Y}). \quad (2.1)$$

Throughout this paper, we use ‘measurability’ to refer to Borel-measurability of a mapping between topological spaces

The absolute continuity of one measure  $\mu \in \mathcal{P}(\mathbb{X})$  with respect to another measure  $\nu$  will be denoted  $\mu \ll \nu$ .

We denote the  $s$ -dimensional Hausdorff measure by  $\mathcal{H}^s$ . If  $E$  is an  $s$ -dimensional set, then  $\mathcal{H}_E$  denotes the restriction of  $\mathcal{H}^s$  to  $E$ .

## 2.1. Gaussian measures on Hilbert spaces

We first briefly recall some basic notions related to measures, especially Gaussian measures, on Hilbert spaces. A standard reference in this area is the book of [Bogachev \(1998\)](#).

In the following, we consider a separable Hilbert space  $\mathbb{H}$  with norm  $\|\cdot\|$  and inner product  $\langle \cdot, \cdot \rangle$ . Suppose  $\mu \in \mathcal{P}(\mathbb{H})$  with finite second moment  $\int_{\mathbb{H}} \|x\|^2 \mu(dx)$  is given. Then the *mean element*  $a \in \mathbb{H}$  and *covariance operator*  $C: \mathbb{H} \rightarrow \mathbb{H}$  of  $\mu$  are determined by

$$0 = \int_{\mathbb{H}} \langle v, x - a \rangle \mu(dx) \quad \text{for all } v \in \mathbb{H}, \quad (2.2)$$

$$\langle Cu, v \rangle = \int_{\mathbb{H}} \langle u, x - a \rangle \langle v, x - a \rangle \mu(dx) \quad \text{for all } u, v \in \mathbb{H}. \quad (2.3)$$

When  $a = 0$ , the measure  $\mu$  is said to be *centred*.

In this paper, we focus on *Gaussian measures*  $\mu = N(a, C)$  on  $\mathbb{H}$ . Such measures are equivalently determined by the property that every one-dimensional linear image is Gaussian on  $\mathbb{R}$ , i.e. identifying  $\ell \in \mathbb{H}$  with the continuous linear functional  $\mathbb{H} \rightarrow \mathbb{R}$ ,  $x \mapsto \langle \ell, x \rangle$ ,

$$\mu = N(a, C) \in \mathcal{P}(\mathbb{H}) \iff \forall \ell \in \mathbb{H}, \ell_{\#}\mu = N(\langle \ell, a \rangle, \langle C\ell, \ell \rangle) \in \mathcal{P}(\mathbb{R});$$

or by the form of the characteristic function, i.e.

$$\mu = N(a, C) \in \mathcal{P}(\mathbb{H}) \iff \forall v \in \mathbb{H}, \int_{\mathbb{H}} \exp(i\langle v, x \rangle) \mu(dx) = \exp(i\langle v, a \rangle - \frac{1}{2}\langle Cv, v \rangle).$$

The covariance operator  $C$  of a probability measure on  $\mathbb{H}$  is always self-adjoint and positive semi-definite, and so its eigenvalues are all real and non-negative. Furthermore, the assumption of finite second moment implies that these eigenvalues are summable, i.e.  $C$  is a trace-class operator.

Given any self-adjoint and positive-definite operator  $C: \mathbb{H} \rightarrow \mathbb{H}$ , we define for  $x, y \in \text{ran}(C^{1/2})$  the weighted inner product and norm

$$\langle x, y \rangle_C := \langle C^{-1/2}x, C^{-1/2}y \rangle, \quad (2.4)$$

$$\|x\|_C := \sqrt{\langle x, x \rangle_C}. \quad (2.5)$$

If  $C$  is the covariance operator of a Gaussian measure  $\mu = N(a, C)$ , then  $\text{ran}(C^{1/2})$  is the *Cameron–Martin space* of  $\mu$ , and (2.4) and (2.5) are often called the *precision* inner product and norm respectively.

The topological support of  $N(0, C)$  — i.e. the smallest closed set of full measure — is the closure in  $\mathbb{H}$  of  $\text{ran}(C)$  (Bogachev, 1998, Theorem 3.6.1). A sufficient condition for the density of  $\text{ran}(C)$  in  $\mathbb{H}$  is the strict positivity of  $C$ , i.e. that it has no null eigenvalue. The containments  $\text{ran}(C) \subseteq \text{ran}(C^{1/2}) \subseteq \mathbb{H}$  always hold, and are strict when the Cameron–Martin space  $\text{ran}(C^{1/2})$  has infinite dimension.

## 2.2. Angular central Gaussian measures on spheres in Hilbert spaces

We denote the unit sphere in a separable Hilbert space  $\mathbb{H}$  by

$$\mathbb{S} := \{\bar{x} \in \mathbb{H} \mid \|\bar{x}\| = 1\}.$$

If  $\mathbb{H} = \mathbb{R}^d$ , then we emphasise the dimension and denote the unit sphere by  $\mathbb{S}^{d-1}$ . The sphere  $\mathbb{S}$  is equipped with the following metric  $d_{\mathbb{S}}: \mathbb{S} \times \mathbb{S} \rightarrow [0, \pi]$ :

$$d_{\mathbb{S}}(\bar{x}, \bar{y}) := \arccos(\langle \bar{x}, \bar{y} \rangle) = 2 \arcsin\left(\frac{1}{2}\|\bar{x} - \bar{y}\|\right) \quad \bar{x}, \bar{y} \in \mathbb{S}, \quad (2.6)$$

where the second identity follows from elementary trigonometry. The definition of  $d_{\mathbb{S}}$  by the arcsine function also extends to the unit sphere  $\mathbb{S}$  in general Banach spaces. Moreover, it yields the Lipschitz equivalence — and hence the topological equivalence — of  $d_{\mathbb{S}}$  and the metric on  $\mathbb{S}$  induced by the norm  $\|\cdot\|$  of the ambient space  $\mathbb{H}$ :

$$\|\bar{x} - \bar{y}\| \leq d_{\mathbb{S}}(\bar{x}, \bar{y}) \leq \frac{\pi}{2}\|\bar{x} - \bar{y}\| \quad \forall \bar{x}, \bar{y} \in \mathbb{S}, \quad (2.7)$$

since  $g(r) = 2 \arcsin(\frac{1}{2}r)/r$  varies between 1 and  $\pi/2$  for  $r \in [0, 2]$ . Thus, the metric  $d_{\mathbb{S}}$  is topologically equivalent to the norm of the ambient space on  $\mathbb{S}$ . We record this result in Lemma A.1. According to Kechris (1995, Proposition 3.3(ii)), a closed subset of a Polish space is always itself Polish in the relative (subspace) topology. Thus,  $(\mathbb{S}, d_{\mathbb{S}})$  is a Polish space and  $\mathcal{B}(\mathbb{S}) = \{B \cap \mathbb{S} \mid B \in \mathcal{B}(\mathbb{H})\}$ .

Fix an arbitrary  $\bar{z} \in \mathbb{S}$ . We denote the radial projection to the sphere by

$$\Pi^{\mathbb{S}}: \mathbb{H} \rightarrow \mathbb{S}, \quad \Pi^{\mathbb{S}}(x) := \begin{cases} \frac{x}{\|x\|}, & \text{if } x \neq 0, \\ \bar{z}, & \text{if } x = 0. \end{cases} \quad (2.8)$$

The choice of  $\bar{z}$  is not important in what follows, but we fix  $\bar{z}$  in order to ensure that  $\Pi^{\mathbb{S}}$  is a measurable mapping from  $\mathbb{H}$  into  $\mathbb{S}$ .

The ACG measure on  $\mathbb{S}$  is now given as follows. Let  $N(0, C)$  be a centred Gaussian measure on  $\mathbb{H}$  and let  $\Pi^{\mathbb{S}}: \mathbb{H} \rightarrow \mathbb{S}$  be as above. Then we call the probability measure

$$\mu := \Pi_{\#}^{\mathbb{S}} N(0, C)$$

the *angular central Gaussian measure* with parameter  $C$  and denote it by  $\mu = \text{ACG}(C)$ . In other words, under  $\text{ACG}(C)$ , each  $E \in \mathcal{B}(\mathbb{S})$  is assigned the Gaussian  $N(0, C)$ -measure of the cone  $\{\alpha u \in \mathbb{X} \mid \alpha > 0, u \in E\}$ . Note that  $\text{ACG}(C) = \text{ACG}(\lambda C)$  for  $\lambda \neq 0$  and so it can sometimes be useful to fix a normalisation for  $C$ , e.g. by taking its leading eigenvalue to be unity.

Whenever  $N(0, C)$  has support equal to  $\mathbb{H}$ , Corollary A.2 immediately implies that the induced  $\text{ACG}(C)$  measure has support equal to  $\mathbb{S}$ ; thus, in view of Section 2.1,  $\text{ACG}(C)$  is a strictly positive measure on  $\mathbb{S}$  whenever  $C$  is positive definite.

In the case where  $\mathbb{H} = \mathbb{R}^d$  with the usual Euclidean norm and  $C \in \mathbb{R}^{d \times d}$  is symmetric and positive definite, one can show that the density  $\rho: \mathbb{S}^{d-1} \rightarrow [0, \infty)$  of  $\mu = \text{ACG}(C)$  with respect to the  $(d-1)$ -dimensional Hausdorff measure on the sphere is

$$\begin{aligned} \rho(\bar{x}) &= \int_0^\infty \frac{\exp(-\frac{1}{2}(r\bar{x}) \cdot C^{-1}(r\bar{x}))}{\sqrt{\det(2\pi C)}} r^{d-1} \, dr \\ &= \frac{\Gamma(d/2)}{2(\frac{1}{2}\|\bar{x}\|_C^2)^{d/2} \sqrt{\det(2\pi C)}} \\ &= \frac{\Gamma(d/2)}{2\pi^{d/2} \sqrt{\det C}} \|\bar{x}\|_C^{-d}. \end{aligned}$$

In the second equation, we used the fact that, for  $a > 0$  and  $n \in \mathbb{N}$ ,  $\int_0^\infty a^{-r^2} r^{n-1} \, dr = \frac{\Gamma(n/2)}{2(\log a)^{n/2}}$ ; see e.g. (Tyler, 1987, Equation (1)).

**Remark 2.1.** The above definitions and properties can be readily adapted to the image of a centred Gaussian measure on a projective space, i.e. the quotient of  $\mathbb{H}$  by the equivalence relation  $u \sim v \iff u = \lambda v$  for some  $\lambda \neq 0$ , i.e.  $\mathbb{S}$  with antipodal points identified. Note that, while  $\text{ACG}(C)$  on  $\mathbb{S}$  is always a multimodal distribution (at best bimodal, if the leading eigenvalue of  $C$  has multiplicity one), its image on the projective space can be unimodal, which may be desirable in applications.

### 3. Markov chain Monte Carlo

Markov chain methods provide a standard tool for approximate sampling of complicated distributions, such as posterior distributions appearing in the Bayesian analysis of data. We recall here notions related to MCMC on a general state space  $\mathbb{X}$  equipped with a target probability measure  $\mu \in \mathcal{P}(\mathbb{X})$ , the Metropolis–Hastings and slice sampling paradigms, and make some particular points about MCMC on infinite-dimensional Hilbert spaces.

#### 3.1. General notions

By a *Markov kernel* on a topological space  $\mathbb{X}$  we mean a function  $K: \mathbb{X} \times \mathcal{B}(\mathbb{X}) \rightarrow [0, 1]$  such that  $K(x, \cdot) \in \mathcal{P}(\mathbb{X})$  for each  $x \in \mathbb{X}$ , and  $K(\cdot, A)$  is a measurable function for each  $A \in \mathcal{B}(\mathbb{X})$ . A sequence of random variables  $(X_n)_{n \in \mathbb{N}}$ , mapping from  $(\Omega, \mathcal{A}, \mathbb{P})$  to  $\mathbb{X}$ , is a (*time-homogeneous*) *Markov chain* with *transition kernel*  $K$  on  $\mathbb{X}$  if

$$\mathbb{P}(X_{n+1} \in A \mid X_1, \dots, X_n) = \mathbb{P}(X_{n+1} \in A \mid X_n) = K(X_n, A), \quad n \in \mathbb{N}, A \in \mathcal{B}(\mathbb{X}),$$

where  $K$  is a Markov kernel<sup>1</sup>. We abuse notation and also use  $K$  to denote the transition operator induced by the kernel  $K$ ; the transition operator acts on functions  $f: \mathbb{X} \rightarrow \mathbb{R}$  via

$$(Kf)(x) := \int_{\mathbb{X}} f(y) K(x, dy) = \mathbb{E}[f(X_{n+1}) \mid X_n = x] \quad \text{for } x \in \mathbb{X}. \quad (3.1)$$

The idea of MCMC is to construct a Markov chain  $(X_n)_{n \in \mathbb{N}}$  with transition kernel  $K$  such that the distribution of  $X_n$  converges to  $\mu$  as  $n \rightarrow \infty$ . Ideally, this convergence will be “fast” and the correlation between successive random variables  $X_n$  and  $X_{n+1}$  will also be weak.

---

<sup>1</sup>In this paper, we shall distinguish between Markov kernels and transition kernels. A transition kernel is a Markov kernel associated to a time-homogeneous Markov chain.

A necessary condition for a transition kernel  $K$  to have  $\mu$  as a limiting distribution is that  $\mu$  is an *invariant distribution* of  $K$ , i.e.

$$\mu(A) = \mu K(A) := \int_{\mathbb{X}} K(x, A) \mu(dx), \quad \text{for all } A \in \mathcal{B}(\mathbb{X}). \quad (3.2)$$

*Reversibility* (or *detailed balance*) of a transition kernel  $K$  on  $\mathbb{X}$  with respect to  $\mu$  refers to the property that

$$K(x, dy)\mu(dx) = K(y, dx)\mu(dy), \quad (3.3)$$

i.e. that the measure  $K(x, dy)\mu(dx)$  on  $\mathbb{X} \times \mathbb{X}$  is symmetric. If (3.3) holds we say that  $K$  is  $\mu$ -reversible. Reversibility of a transition kernel  $K$  with respect to  $\mu$  implies that  $K$  has  $\mu$  as an invariant distribution, although the converse is generally false.

If  $\mu$  is an invariant distribution of  $K$ , and if some non-restrictive regularity conditions such as  $\varphi$ -irreducibility and Harris recurrence hold, then a strong law of large numbers holds, i.e.

$$\lim_{n \rightarrow \infty} \frac{1}{N} \sum_{n=1}^N f(X_n) = \int_{\mathbb{X}} f(x) \mu(dx) \quad \mathbb{P}\text{-a.s.},$$

for any  $\mu$ -integrable  $f: \mathbb{X} \rightarrow \mathbb{R}$  (Meyn and Tweedie, 2009; Asmussen and Glynn, 2011). This shows that the ‘‘MCMC-time average’’  $\frac{1}{N} \sum_{n=1}^N f(X_n)$  can be used to approximate the mean of  $f$  with respect to the distribution of interest  $\mu$ . For more quantitative statements the spectral gap of a Markov chain (or its transition kernel) is a crucial quantity. For a transition kernel  $K$  that is reversible with respect to  $\mu$  (inducing the transition operator  $K$  via (3.1)) we define

$$\text{gap}_{\mu}(K) := 1 - \|K\|_{L_{0,\mu}^2 \rightarrow L_{0,\mu}^2}, \quad (3.4)$$

where  $L_{0,\mu}^2$  denotes the space of square integrable and mean zero functions  $f: \mathbb{X} \rightarrow \mathbb{R}$  with respect to  $\mu$ . An  $L_{\mu}^2$ -spectral gap, that is,  $\text{gap}_{\mu}(K) > 0$ , leads to desirable properties of a Markov chain  $(X_n)_{n \in \mathbb{N}}$  with transition kernel  $K$ . For instance, it implies a central limit theorem, see e.g. (Douc et al., 2018, Section 22.5) and the relevant references therein. In particular, an explicit lower bound on  $\text{gap}_{\mu}(K)$  leads to an estimate of the total variation distance and a mean squared error bound of the time average  $\frac{1}{N} \sum_{n=1}^N f(X_n)$ . More precisely, it is well known, e.g. by virtue of (Novak and Rudolf, 2014, Lemma 2 and Lemma 3), that

$$\|\xi K^n - \mu\|_{\text{TV}} \leq (1 - \text{gap}_{\mu}(K))^n \left\| \frac{d\xi}{d\mu} - 1 \right\|_{2,\mu}, \quad (3.5)$$

where  $\|\xi K^n - \mu\|_{\text{TV}} := \sup_{A \in \mathcal{B}(\mathbb{X})} |\xi K^n(A) - \mu(A)|$  denotes the total variation distance between  $\xi K^n = \mathbb{P}_{X_{n+1}}$  and  $\mu$ ,  $\xi := \mathbb{P}_{X_1}$ , and  $\|f\|_{p,\mu}^p := \int_{\mathbb{X}} |f|^p d\mu$  for  $f: \mathbb{X} \rightarrow \mathbb{R}$ . Furthermore, Rudolf (2012) shows that for every  $p > 2$ , there exists an explicit constant  $c_p$  such that for  $f \in L^p(\mu)$  with  $\|f\|_{p,\mu}^p \leq 1$ ,

$$\mathbb{E} \left[ \left| \frac{1}{N} \sum_{n=1}^N f(X_n) - \int_{\mathbb{X}} f d\mu \right|^2 \right] \leq \frac{2}{N \cdot \text{gap}_{\mu}(K)} + \frac{c_p \left\| \frac{d\xi}{d\mu} - 1 \right\|_{\infty}}{N^2 \cdot \text{gap}_{\mu}(K)^2}.$$

There are also other non-asymptotic bounds that consider different convergence assumptions on the Markov chain and the underlying error criterion. For details we refer to (Łatuszyński and Niemiro, 2011; Łatuszyński et al., 2013; Rudolf and Schweizer, 2015; Paulin, 2015; Fan et al., 2021) and the references therein.

In the following we briefly discuss two popular methods for the construction of a transition kernel  $K$  that is reversible with respect to  $\mu$ .

### 3.2. Metropolis–Hastings (MH) algorithms

Probably the most popular method for constructing a transition kernel that is reversible with respect to  $\mu$  is given by the MH algorithm. Given a Markov kernel  $Q$  on  $\mathbb{X}$  which serves as a proposal mechanism (i.e. a ‘proposal kernel’) and given a function  $\alpha: \mathbb{X} \times \mathbb{X} \rightarrow [0, 1]$  which provides acceptance probabilities and depends on  $\mu$  and  $Q$ , a transition from a state  $x$  to a state  $y$  in the MH algorithm proceeds as follows.

**Transition mechanism 3.1** (Metropolis–Hastings). Let  $Q$  be a proposal kernel and  $\alpha: \mathbb{X} \times \mathbb{X} \rightarrow [0, 1]$  be an acceptance probability function. Given the current state  $x \in \mathbb{X}$ , one obtains the next state  $y \in \mathbb{X}$  as follows:

- (1) Draw  $X' \sim Q(x, \cdot)$  and  $U \sim \text{U}[(0, 1)]^2$  independently and denote the realisations by  $x'$  and  $u$  respectively;
- (2) If  $u < \alpha(x, x')$ , return  $y := x'$ , otherwise return  $y := x$ .

The algorithm above can be rewritten as a transition kernel:

$$K(x, dy) = \alpha(x, y)Q(x, dy) + r(x)\delta_x(dy), \quad r(x) := 1 - \int_{\mathbb{X}} \alpha(x, y)Q(x, dy), \quad (3.6)$$

where  $\delta_x$  denotes the Dirac measure on  $\mathbb{X}$  at  $x \in \mathbb{X}$  and the function  $r$  is called the ‘rejection probability’. It remains to specify  $\alpha$ . Let  $\sigma^+, \sigma^- \in \mathcal{P}(\mathbb{X} \times \mathbb{X})$  with

$$\begin{aligned} \sigma^+(dx, dx') &:= Q(x, dx')\mu(dx), \\ \sigma^-(dx, dx') &:= \sigma^+(dx', dx) = Q(x', dx)\mu(dx'), \end{aligned} \quad (3.7)$$

and set

$$\alpha(x, x') := \min \left\{ 1, \frac{d\sigma^-}{d\sigma^+}(x, x') \right\}.$$

Then the transition kernel  $K$  defined in (3.6) is reversible with respect to  $\mu$  (Tierney, 1998). Of course, the Radon–Nikodym derivative  $\frac{d\sigma^-}{d\sigma^+}(x, x')$  does not necessarily exist. In the finite-dimensional Euclidean setting where  $\mathbb{X} = \mathbb{R}^d$ , the derivative  $\frac{d\sigma^-}{d\sigma^+}$  is often just the ratio of Lebesgue densities. However, in infinite-dimensional spaces the absolute continuity  $\sigma^- \ll \sigma^+$  requires the choice of a suitable proposal kernel  $Q$ .

### 3.3. Slice sampling

Suppose that a  $\sigma$ -finite reference measure  $\mu_0$  on  $\mathbb{X}$  is given that satisfies  $\mu \ll \mu_0$ . Additionally, we assume that the probability density function  $\frac{d\mu}{d\mu_0}$  satisfies

$$\frac{d\mu}{d\mu_0}(x) \propto \exp(-\Phi(x)), \quad \mu_0\text{-a.e. } x \in \mathbb{X},$$

for a measurable function  $\Phi: \mathbb{X} \rightarrow \mathbb{R}$  such that  $\exp(-\Phi)$  is integrable with respect to  $\mu_0$ . For some  $s > 0$ , define

$$\mathbb{X}_s := \{x \in \mathbb{X} \mid \exp(-\Phi(x)) \geq s\}, \quad (3.8)$$

to be the super-level set of  $\exp(-\Phi)$  to level  $s$ . Let  $\|\exp(-\Phi)\|_\infty := \mu_0\text{-ess sup}_{x \in \mathbb{X}} |\exp(-\Phi(x))|$  and note that  $\mu_0(\mathbb{X}_s) \in (0, \infty)$  for  $s \in (0, \|\exp(-\Phi)\|_\infty)$ . Define the probability measure  $\mu_{0,s} \in \mathcal{P}(\mathbb{X})$  by

$$\mu_{0,s}(A) := \frac{\mu_0(A \cap \mathbb{X}_s)}{\mu_0(\mathbb{X}_s)}, \quad A \in \mathcal{B}(\mathbb{X}),$$

---

<sup>2</sup>We denote the uniform distribution on  $G \subset \mathbb{R}^d$  by  $\text{U}[G]$ .



that is,  $\mu_{0,s}$  is the normalised restriction of  $\mu_0$  to  $\mathbb{X}_s$ . In the idealised slice sampling algorithm, a transition from a state  $x$  to a state  $y$  proceeds as follows.

**Transition mechanism 3.2** (Idealised slice sampling). Given the current state  $x \in \mathbb{X}$  one obtains the next state  $y \in \mathbb{X}$  as follows:

- (1) Draw  $S \sim \text{U}[(0, \exp(-\Phi(x)))]$  and let  $s$  be the realisation.
- (2) Draw  $Y \sim \mu_{0,s}$  and let the state  $y$  be the realisation of  $Y$ .

The corresponding transition kernel takes the form

$$K(x, dy) = \frac{1}{\exp(-\Phi(x))} \int_0^{\exp(-\Phi(x))} \mu_{0,s}(dy) ds,$$

and it can be readily shown that  $K$  is reversible with respect to  $\mu$ .

**Remark 3.3.** In the case that  $\mathbb{X} = \mathbb{R}^d$  and  $\mu_0$  is the Lebesgue measure,  $\mu_{0,s}$  coincides with the uniform distribution on  $\mathbb{X}_s$ . In that setting the corresponding methodology is known as simple (uniform) slice sampling and recent results (Natarovskii et al., 2021b, Theorem 3.10) concerning the spectral gap indicate under which conditions robust convergence behavior with respect to the dimension is present.

However, the main issue with the idealised slice sampling algorithm is that the second step in [Transition mechanism 3.2](#) may be difficult to implement, because the implicit assumption of being able to draw samples from  $\mu_{0,s}$  for an arbitrary level  $s$  may be very restrictive. Whenever one is not able to sample from a distribution exactly, one can try to use a suitable Markov chain step. Namely, one substitutes the second step of [Transition mechanism 3.2](#) by performing a transition, depending on  $x$  and  $t$ , which (at least) has stationary distribution  $\mu_{0,s}$ . Such approaches are known as *hybrid slice sampling* strategies; see e.g. (Łatuszyński and Rudolf, 2014) for some theory and comparison results. There are several different methods in the literature that are feasible in finite-dimensional settings, and can — from an algorithmic perspective — be lifted to infinite-dimensional scenarios; see e.g. (Neal, 2003; Murray et al., 2010; Li and Walker, 2020).

### 3.4. MCMC in Hilbert spaces

We consider the case where  $\mathbb{X}$  is a separable Hilbert space denoted by  $\mathbb{H}$  and where the target/posterior distribution  $\nu \in \mathcal{P}(\mathbb{H})$  is determined by a density with respect to a Gaussian reference/prior measure  $\nu_0 = \text{N}(0, C)$ , that is,

$$\frac{d\nu}{d\nu_0}(x) \propto \exp(-\Phi(x)), \quad \nu_0\text{-a.e. } x \in \mathbb{H}, \quad (3.9)$$

with measurable  $\Phi: \mathbb{H} \rightarrow \mathbb{R}$  satisfying

$$\int_{\mathbb{H}} \exp(-\Phi(x)) \nu_0(dx) < \infty.$$

In this setting we state two popular approaches for generating  $\nu$ -reversible Markov chains. The first is the pCN-MH algorithm (Neal, 1999; Cotter et al., 2013). Here  $s \in (0, 1]$  is a given step size parameter. Using the notation of [Transition mechanism 3.1](#), the pCN-MH proposal kernel  $Q$  takes the form

$$Q(x, dy) := \text{N}(\sqrt{1-s^2}x, s^2C),$$

---

**Algorithm 1.** pCN-MH algorithm on  $\mathbb{H}$ 


---

```

1: Given: prior  $\nu_0 = \mathcal{N}(0, C)$  and target  $\nu$  as in (3.9)
2: Initial: step size  $s \in (0, 1]$  and state  $x_0 \in \mathbb{H}$ 
3: for  $k \in \mathbb{N}_0$  do
4:   Draw a sample  $w_k$  of  $\mathcal{N}(0, C)$  and set  $y_{k+1} := \sqrt{1 - s^2}x_k + sw_k$ 
5:   Compute  $\alpha := \min\{1, \exp(\Phi(x_k) - \Phi(y_{k+1}))\}$ 
6:   Draw a sample  $u$  of  $\mathcal{U}[0, 1]$ 
7:   if  $u \leq \alpha$  then
8:     Set  $x_{k+1} = y_{k+1}$ 
9:   else
10:    Set  $x_{k+1} = x_k$ 
11:   end if
12: end for

```

---

and the acceptance probability function  $\alpha$  simplifies to

$$\alpha(x, y) := \min\{1, \exp(\Phi(x) - \Phi(y))\}.$$

Substituting the pCN-MH proposal kernel  $Q$  and the MH acceptance probability function  $\alpha$  in (3.6) yields the pCN-MH transition kernel. Algorithm 1 describes how to realise a Markov chain with pCN-MH transition kernel.

Next, we consider the ESS algorithm suggested in (Murray et al., 2010). In this reference it is stated in a finite-dimensional setting, but the ESS algorithm can be lifted also to infinite-dimensional settings. In the framework of Transition mechanism 3.2, we have  $\mu_0 = \nu_0 = \mathcal{N}(0, C)$ , and for  $s > 0$ ,  $\mu_{0,s}$  is a truncated Gaussian restricted to the level set  $\mathbb{H}_s$  (cf. (3.8)). Elliptical slice sampling is a hybrid slice sampler, i.e. rather than performing the second step of Transition mechanism 3.2, a transition is used that mimics the sampling with respect to  $\mu_{0,s}$ . We state this transition in Algorithm 2, which we call *shrink-ellipse*( $x, t$ ). Here,  $x$  and  $t$  denote the current state and current level respectively.

---

**Algorithm 2.** Elliptical shrinkage (*shrink-ellipse*( $x, t$ ))

---

```

1: Input: state  $x \in \mathbb{H}$  and level  $t \in (0, \infty)$ 
2: Output: state  $y$  in level set  $\mathbb{H}_t$ 
3: Draw a sample  $w \sim \mathcal{N}(0, C)$ 
4: Draw a sample  $\theta \sim \mathcal{U}[0, 2\pi]$ 
5: Set  $\theta_{\min} = \theta - 2\pi$  and  $\theta_{\max} = \theta$ 
6: while  $\exp(\Phi(y)) < t$  do
7:   if  $\theta < 0$  then
8:     Set  $\theta_{\min} = \theta$ 
9:   else
10:    Set  $\theta_{\max} = \theta$ 
11:   end if
12:   Draw a sample  $\theta \sim \mathcal{U}[\theta_{\min}, \theta_{\max}]$ 
13:   Set  $y = \cos(\theta)x + \sin(\theta)w$ 
14: end while

```

---

Substituting the *shrink-ellipse*( $x, t$ ) algorithm in the second step of Transition mechanism 3.2 leads to a transition kernel that has  $\nu$  as invariant distribution; see (Murray et al., 2010) and

(Natarovskii, 2021, Section 3) for further details. In particular, in Algorithm 3 we describe how to realise a Markov chain with ESS transition kernel.

---

**Algorithm 3.** ESS algorithm on  $\mathbb{H}$

---

- 1: **Given:** prior  $\nu_0 = N(0, C)$  and target  $\nu$  as in (3.9)
  - 2: **Initial:** state  $x_0 \in \mathbb{H}$
  - 3: **for**  $k \in \mathbb{N}_0$  **do**
  - 4:   Draw sample  $t \sim U[0, \exp(-\Phi(x_k))]$
  - 5:   Set  $x_{k+1} = \text{shrink-ellipse}(x_k, t)$  (see Algorithm 2)
  - 6: **end for**
- 

**Remark 3.4.** As noted in (Murray et al., 2010), both the ESS algorithm and the pCN algorithm draw proposal states from ellipses that are accepted or rejected. In the pCN algorithm, the random proposal  $X'$  satisfies  $X' = \sqrt{1-s^2}x + sZ$ , where  $Z \sim N(0, C)$ . For a fixed realisation  $z$  of  $Z$  and for varying  $s \in (0, 1)$ , the set  $\{\sqrt{1-s^2}x + sz \mid s \in (0, 1)\}$  is half of the ellipse passing through  $x$  and  $z$  centred at the origin, since  $\sqrt{1-s^2}x + sz = \cos(\theta)x + \sin(\theta)z$  for  $\theta = \arcsin(s)$ . In the elliptical slice sampling algorithm, a full ellipse instead of a half ellipse is used, thus providing a larger set of potential proposal states. Moreover, one never remains at the current state. Intuitively, using a larger set of potential proposal states might lead to faster convergence, as measured by the number of Markov chain steps.

## 4. Markov chain Monte Carlo on the sphere

In this section, we construct and analyse MCMC algorithms for approximate sampling from a probability distribution on a high-dimensional sphere, where the distribution admits a density with respect to an ACG reference or prior measure. Our algorithms exploit the fact that the ACG prior can be lifted to the ambient Hilbert space. This lifting property allows us to use suitable MCMC methods on high- or infinite-dimensional Hilbert spaces, e.g. those that we described in the previous section.

Suppose we are given a target or posterior measure  $\mu \in \mathcal{P}(\mathbb{S})$  on the unit sphere  $\mathbb{S}$  of a Hilbert space  $\mathbb{H}$  and a measurable function  $\bar{\Phi}: \mathbb{S} \rightarrow \mathbb{R}$  that satisfies

$$\int_{\mathbb{S}} \exp(-\bar{\Phi}(\bar{x})) \mu_0(d\bar{x}) < \infty.$$

Suppose that  $\mu$  is absolutely continuous with respect to an ACG reference or prior measure  $\mu_0 := \text{ACG}(C)$ , and

$$\frac{d\mu}{d\mu_0}(\bar{x}) \propto \exp(-\bar{\Phi}(\bar{x})), \quad \bar{x} \in \mathbb{S}. \quad (4.1)$$

The ACG prior allows us to define an equivalent sampling problem in the ambient Hilbert space.

**Lifting to ambient Hilbert space.** Define the measurable function  $\Phi: \mathbb{H} \rightarrow \mathbb{R}$  by

$$\Phi(x) := \bar{\Phi}(\Pi^{\mathbb{S}}(x)), \quad x \in \mathbb{H}, \quad (4.2)$$

where  $\Pi^{\mathbb{S}}: \mathbb{H} \rightarrow \mathbb{S}$  is the radial projection to the sphere (2.8), and define a target measure  $\nu \in \mathcal{P}(\mathbb{H})$  via

$$\frac{d\nu}{d\nu_0}(x) \propto \exp(-\Phi(x)), \quad \nu_0\text{-a.e. } x \in \mathbb{H}, \quad (4.3)$$

where  $\nu_0 = \mathcal{N}(0, C)$ . Using  $\mu_0 = \text{ACG}(C) = \Pi_{\sharp}^{\mathbb{S}} \nu_0$  and using the construction of  $\Phi$ , we obtain  $\mu = \Pi_{\sharp}^{\mathbb{S}} \nu$ . We show this result in a slightly more general form, i.e. for an arbitrary measurable map  $T: \mathbb{X} \rightarrow \mathbb{Y}$  between two arbitrary topological spaces  $\mathbb{X}$  and  $\mathbb{Y}$ :

**Proposition 4.1.** *Let  $\nu_0 \in \mathcal{P}(\mathbb{X})$ , let  $T: \mathbb{X} \rightarrow \mathbb{Y}$  be measurable, and let  $\bar{\Phi}: \mathbb{Y} \rightarrow \mathbb{R}$  be such that  $Z = \int_{\mathbb{Y}} \exp(-\bar{\Phi}(T(x))) \nu_0(dx) < \infty$ . Define  $\nu$  by*

$$\frac{d\nu}{d\nu_0}(x) = \frac{1}{Z} \exp(-\bar{\Phi}(T(x))), \quad \nu_0\text{-a.e. } x \in \mathbb{X}.$$

Then

$$\frac{dT_{\sharp}\nu}{dT_{\sharp}\nu_0}(\bar{x}) = \frac{1}{Z} \exp(-\bar{\Phi}(\bar{x})), \quad T_{\sharp}\nu_0\text{-a.e. } \bar{x} \in \mathbb{Y}.$$

**Proof.** Let  $A \in \mathcal{B}(\mathbb{Y})$ . We shall show that

$$(T_{\sharp}\nu)(A) = \frac{1}{Z} \int_A \exp(-\bar{\Phi}(\bar{x})) T_{\sharp}\nu_0(d\bar{x}). \quad (4.4)$$

To this end, let  $X \sim \nu_0$  and  $\bar{X} := T(X)$ , i.e.  $\bar{X} \sim T_{\sharp}\nu_0$ , be random variables on the underlying probability space  $(\Omega, \mathcal{A}, \mathbb{P})$  that we fixed in [Section 2](#). Then

$$\begin{aligned} (T_{\sharp}\nu)(A) &= \frac{1}{Z} \int_{T^{-1}(A)} \exp(-\bar{\Phi}(T(x))) \nu_0(dx) \\ &= \frac{1}{Z} \int_{X^{-1}(T^{-1}(A))} \exp(-\bar{\Phi}(T(X(\omega)))) \mathbb{P}(d\omega) && \text{since } \nu_0 = \mathbb{P} \circ X^{-1} \\ &= \frac{1}{Z} \int_{\bar{X}^{-1}(A)} \exp(-\bar{\Phi}(\bar{X}(\omega))) \mathbb{P}(d\omega) && \text{since } \bar{X} := T(X) \\ &= \frac{1}{Z} \int_A \exp(-\bar{\Phi}(\bar{x})) T_{\sharp}\nu_0(d\bar{x}) && \text{since } \bar{X} \sim T_{\sharp}\nu_0, \end{aligned}$$

which establishes (4.4) and completes the proof.  $\blacksquare$

The insight that we need to sample the push-forward  $\mu = T_{\sharp}\nu$  of a measure  $\nu$  defined on the ambient Hilbert space  $\mathbb{H}$  is crucial for the construction of the following algorithms. In particular, we shall exploit suitable transition kernels for sampling from  $\nu \in \mathcal{P}(\mathbb{H})$  in order to construct Markov chains on  $\mathbb{S}$  with invariant distribution  $T_{\sharp}\nu$ , where  $T = \Pi^{\mathbb{S}}$ . To this end, we use the methodology of push-forward transition kernels, which we describe in the next subsection.

#### 4.1. The reprojection method

We present now a simple method for defining a  $\mu$ -reversible Markov chain  $(\bar{X}_n)_{n \in \mathbb{N}}$  on  $\mathbb{S}$ , by using a  $\nu$ -reversible transition kernel  $K$  on  $\mathbb{H}$ . The method employs the concept of *push-forward transition kernels* which we explain for the general setting of Polish spaces  $\mathbb{X}, \mathbb{Y}$  connected via a measurable mapping  $T: \mathbb{X} \rightarrow \mathbb{Y}$ . For more details of this approach we refer to [\(Rudolf and Sprungk, 2022\)](#). For the particular algorithms that we consider later, we focus on the specific case of  $\mathbb{Y} = \mathbb{S}$ ,  $\mathbb{X} = \mathbb{H}$ , and  $T$  the radial projection map  $T = \Pi^{\mathbb{S}}$  given in [\(2.8\)](#).

Given a  $\nu$ -invariant transition kernel  $K$  on  $\mathbb{X}$  and a measurable map  $T: \mathbb{X} \rightarrow \mathbb{Y}$ , we define the *push-forward transition kernel*  $T_{\sharp}K$  on  $\mathbb{Y}$  as follows:

$$T_{\sharp}K(\bar{x}, A) := \mathbb{E}[K(X, T^{-1}(A)) \mid T(X) = \bar{x}], \quad X \sim \nu, \quad (4.5)$$

where  $\bar{x} \in \mathbb{Y}$  and  $A \in \mathcal{B}(\mathbb{Y})$ . If  $T$  is bijective, then

$$T_{\#}K(\bar{x}, A) = K(T^{-1}(\bar{x}), T^{-1}(A)).$$

In the following, we also use the shorter notation  $\bar{K} = T_{\#}K$ . Below, we summarise some important properties of push-forward transition kernels that are inherited from the original transition kernel.

**Lemma 4.2** (Rudolf and Sprungk, 2022). *Let  $\mathbb{X}$  and  $\mathbb{Y}$  be Polish spaces,  $T: \mathbb{X} \rightarrow \mathbb{Y}$  be a measurable mapping,  $K$  be a  $\nu$ -invariant transition kernel on  $\mathbb{X}$ , and  $\mu := T_{\#}\nu$ .*

- (a) *If  $K$  is reversible with respect to  $\nu$ , then  $T_{\#}K$  is reversible with respect to  $\mu$ .*
- (b) *If  $K$  has an  $L^2_{\nu}$ -spectral gap, then  $T_{\#}K$  has an  $L^2_{\mu}$ -spectral gap and*

$$\text{gap}_{\mu}(T_{\#}K) \geq \text{gap}_{\nu}(K).$$

- (c) *If  $K$  is a MH kernel with proposal kernel  $Q: \mathbb{X} \times \mathcal{B}(\mathbb{X}) \rightarrow [0, 1]$  and acceptance probability  $\alpha: \mathbb{X} \times \mathbb{X} \rightarrow [0, 1]$  such that*

$$\alpha(x, y) = \bar{\alpha}(T(x), T(y)) \quad \forall x, y \in \mathbb{X}$$

*for a measurable  $\bar{\alpha}: \mathbb{Y} \times \mathbb{Y} \rightarrow [0, 1]$ , then  $T_{\#}K$  is a MH kernel with acceptance probability  $\bar{\alpha}$  and proposal kernel  $\bar{Q}$  given by*

$$\bar{Q}(\bar{x}, A) := \int_{\mathbb{X}} Q(x, T^{-1}(A)) \nu_{|T}(\bar{x}, dx), \quad \forall \bar{x} \in \mathbb{Y}, A \in \mathcal{B}(\mathbb{Y}),$$

*where  $\nu_{|T}(\bar{x}, \cdot)$  denotes the regular conditional distribution of  $X \sim \nu$  given  $T(X) = \bar{x}$ .*

The last item in the above lemma also shows that one can simulate push-forward transition kernels by exploiting the regular conditional distribution  $\nu_{|T}: \mathbb{Y} \times \mathcal{B}(\mathbb{X}) \rightarrow [0, 1]$  of  $X \sim \nu$  given  $T(X) = \bar{x}$ . We recall that  $\nu_{|T}$  possesses the properties of a transition kernel and satisfies

$$\nu_{|T}(T(X), A) = \mathbb{P}(X \in A \mid T(X)) \quad \mathbb{P}\text{-almost surely}, \quad (4.6)$$

for any  $A \in \mathcal{B}(\mathbb{X})$ . Given this regular conditional distribution, the disintegration theorem yields the representation

$$T_{\#}K(\bar{x}, A) = \int_{\mathbb{X}} K(x, T^{-1}(A)) \nu_{|T}(\bar{x}, dx), \quad (4.7)$$

for general transition kernels  $K$ . Thus, the push-forward transition kernel  $T_{\#}K$  can be realised by the following mechanism.

**Transition mechanism 4.3.** Given the current state  $\bar{x} \in \mathbb{Y}$  one obtains the next state  $\bar{y} \in \mathbb{Y}$  as follows:

- (1) Draw  $X \sim \nu_{|T}(\bar{x}, \cdot)$  and call the realisation  $x \in \mathbb{X}$ ;
- (2) Draw  $Y \sim K(x, \cdot)$ , call the realisation  $y \in \mathbb{X}$  and return  $\bar{y} := T(y) \in \mathbb{Y}$ .

We now consider the specific case of  $\mathbb{X} = \mathbb{H}$  being a Hilbert space,  $\mathbb{Y} = \mathbb{S}$  its unit sphere and  $T = \Pi^{\mathbb{S}}$  being the radial projection defined in (2.8). In order to get a  $\mu$ -reversible Markov chain on  $\mathbb{S}$ , we can consider the push-forward transition kernels  $\bar{K} = T_{\#}K$  of  $\nu$ -reversible transition kernels  $K$  on the ambient Hilbert space  $\mathbb{H}$  — such as the pCN-MH kernel or the ESS kernel — provided that we can also simulate the regular conditional distribution  $\nu_{|T}$  for the lifted target  $\nu$  in (4.3). The resulting algorithm is illustrated in Figure 4.1. In particular, by going randomly from  $\bar{x}$  to  $x$  in the ambient space, performing a transition from  $x$  to  $y$  by using  $K$ , and then by “reprojecting” deterministically from  $y$  to  $\bar{y} = \Pi^{\mathbb{S}}(y)$ , we end up on the sphere  $\mathbb{S}$ . Since this is performed at each iteration of the Markov chain, we name this the *reprojection method*.

Next, we derive the regular conditional distribution  $\nu_{|\Pi^{\mathbb{S}}}$  for Gaussian measures  $\nu = N(0, C)$  on  $\mathbb{H} = \mathbb{R}^d$ , and state the resulting reprojected pCN-MH algorithm as well as the reprojected ESS algorithm.

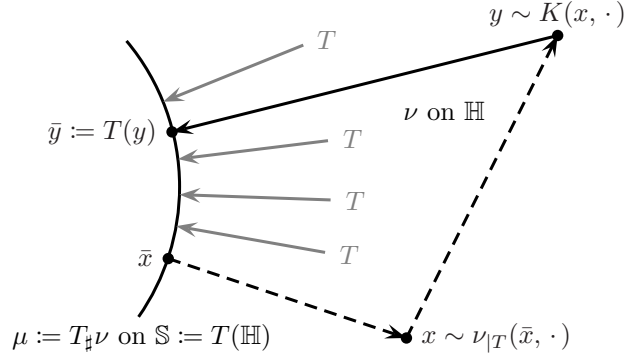


**Figure 4.1.:** Illustration of the steps in the reprojection method from [Section 4.1](#). The reprojection method defines a  $\mu$ -reversible transition kernel on  $\mathbb{S}$  in terms of a  $\nu$ -reversible transition kernel  $K$  on the ambient space  $\mathbb{H}$ , where  $\mathbb{S} := T(\mathbb{H})$ ,  $\mu := T_{\#}\nu$ ,  $\nu_{|T}(\bar{x}, \cdot)$  is the regular conditional distribution of  $X \sim \nu$  given  $T(X) = \bar{x}$ , and  $T = \Pi^{\mathbb{S}}$ . Solid arrows indicate deterministic maps, whereas dashed arrows indicate randomised maps, i.e. draws from transition kernels.

**Simulating the conditional distribution  $\nu_{|\Pi^{\mathbb{S}}}$ .** We first prove a proposition about the regular conditional distributions  $\nu_{|T}$  in the more general setting of Polish spaces  $\mathbb{X}, \mathbb{Y}$ . We then apply this proposition to derive an explicit description for  $\nu_{|\Pi^{\mathbb{S}}}$ .

**Proposition 4.4.** *Let  $\mathbb{X}$  and  $\mathbb{Y}$  be Polish spaces equipped with a measurable mapping  $T: \mathbb{X} \rightarrow \mathbb{Y}$  and  $\nu_0 \in \mathcal{P}(\mathbb{X})$ . Let  $\bar{\Phi}: \mathbb{Y} \rightarrow \mathbb{R}$  be measurable with  $Z := \int_{\mathbb{Y}} \exp(-\bar{\Phi}(T(x))) \nu_0(dx) < \infty$ , define  $\Phi: \mathbb{X} \rightarrow \mathbb{R}$  by  $\Phi(x) := \bar{\Phi}(T(x))$  for  $x \in \mathbb{X}$ , and let  $\nu \in \mathcal{P}(\mathbb{X})$  be given by*

$$\frac{d\nu}{d\nu_0}(x) = \frac{1}{Z} \exp(-\Phi(x)), \quad \nu_0\text{-a.e. } x \in \mathbb{X}.$$

Furthermore, let  $\nu_{0|T}$  be the regular conditional distribution of  $X_0 \sim \nu_0$  given  $T(X_0)$ , and let  $\nu_{|T}$  be the regular conditional distribution of  $X \sim \nu$  given  $T(X)$ . Then

$$\nu_{|T}(T(x), \cdot) = \nu_{0|T}(T(x), \cdot)$$

for  $\nu_0$ -almost every  $x \in \mathbb{X}$ .

The hypotheses of the proposition differ from the hypotheses of [Proposition 4.1](#) only in the additional assumption that  $\mathbb{X}$  and  $\mathbb{Y}$  are Polish spaces. This assumption ensures that we may apply the disintegration theorem to obtain regular conditional distributions. We can weaken the assumption by requiring only that  $\mathbb{X}$  and  $\mathbb{Y}$  are Radon spaces.

**Proof of Proposition 4.4.** The regular conditional distribution  $\nu_{0|T}: \mathbb{Y} \times \mathcal{B}(\mathbb{X}) \rightarrow [0, 1]$  of  $X_0$  given  $T(X_0)$  is defined as a Markov kernel satisfying for every  $A \in \mathcal{B}(\mathbb{X})$  and  $B \in \mathcal{B}(\mathbb{Y})$ ,

$$\mathbb{P}(X_0 \in A, T(X_0) \in B) = \int_B \nu_{0|T}(y, A) T_{\#}\nu_0(dy) = \int_{T^{-1}(B)} \nu_{0|T}(T(x), A) \nu_0(dx).$$

Moreover, given the regular conditional distribution  $\nu_{0|T}$  we can express the conditional expectation of  $g(X_0)$  given  $T(X_0)$  for any measurable  $g: \mathbb{X} \rightarrow \mathbb{R}$  as

$$\mathbb{E}[g(X_0) | T(X_0)] = \int_{\mathbb{X}} g(x) \nu_{0|T}(T(X_0), dx) \quad \text{almost surely.} \quad (4.8)$$

We ask now for the regular conditional distribution  $\nu_{|T}$  of  $X \sim \nu$  given  $T(X)$ . Analogously, this is a Markov kernel  $\nu_{|T}: \mathbb{Y} \times \mathcal{B}(\mathbb{X}) \rightarrow [0, 1]$  satisfying

$$\mathbb{P}(X \in A, T(X) \in B) = \int_B \nu_{|T}(y, A) T_{\#} \nu(dy) = \int_{T^{-1}(B)} \nu_{|T}(T(x), A) \nu(dx)$$

for every  $A \in \mathcal{B}(\mathbb{X})$  and  $B \in \mathcal{B}(\mathbb{Y})$ . Since  $\mathbb{P}(X \in A, T(X) \in B) = \nu(A \cap T^{-1}(B))$  the statement follows, if

$$\nu(A \cap T^{-1}(B)) = \int_{T^{-1}(B)} \nu_{0|T}(T(x), A) \nu(dx) \quad \forall A \in \mathcal{B}(\mathbb{X}) \quad \forall B \in \mathcal{B}(\mathbb{Y}), \quad (4.9)$$

because  $\nu_{0|T}$  is then a valid regular conditional distribution of  $X \sim \nu$  given  $T(X)$ . For  $A \in \mathcal{B}(\mathbb{X}), B \in \mathcal{B}(\mathbb{Y})$  we have

$$\nu(A \cap T^{-1}(B)) = \int_{\mathbb{X}} \mathbb{1}_A(x) \mathbb{1}_B(T(x)) \frac{1}{Z} e^{-\Phi(x)} \nu_0(dx) = \mathbb{E} \left[ \frac{1}{Z} e^{-\Phi(X_0)} \mathbb{1}_A(X_0) \mathbb{1}_B(T(X_0)) \right],$$

where  $X_0 \sim \nu_0$ . Using the law of total expectation and the hypothesis that  $\Phi(x) = \bar{\Phi}(T(x))$  for every  $x \in \mathbb{X}$ , we obtain

$$\begin{aligned} \nu(A \cap T^{-1}(B)) &= \mathbb{E} \left[ \mathbb{E} \left[ \frac{1}{Z} e^{-\Phi(X_0)} \mathbb{1}_A(X_0) \mathbb{1}_B(T(X_0)) \mid T(X_0) \right] \right] \\ &= \mathbb{E} \left[ \frac{1}{Z} e^{-\Phi(X_0)} \mathbb{1}_B(T(X_0)) \mathbb{E}[\mathbb{1}_A(X_0) \mid T(X_0)] \right]. \end{aligned}$$

Applying now (4.8) to  $g(x) = \mathbb{1}_A(x)$  yields  $\mathbb{E}[\mathbb{1}_A(X_0) \mid T(X_0)] = \nu_{0|T}(T(X_0), A)$  and, thus,

$$\begin{aligned} \nu(A \cap T^{-1}(B)) &= \mathbb{E} \left[ \frac{1}{Z} e^{-\Phi(X_0)} \mathbb{1}_B(T(X_0)) \nu_{0|T}(T(X_0), A) \right] \\ &= \int_{T^{-1}(B)} \frac{1}{Z} e^{-\Phi(x)} \nu_{0|T}(T(x), A) \nu_0(dx) \\ &= \int_{T^{-1}(B)} \nu_{0|T}(T(x), A) \nu(dx) \end{aligned}$$

which shows (4.9). ■

We now turn to the setting of a finite dimensional sphere, where  $\mathbb{X} = \mathbb{R}^d$ ,  $\mathbb{Y} = \mathbb{S}^{d-1}$ , and  $T = \Pi^{\mathbb{S}}$ . In order to implement the reprojection method, it suffices by [Proposition 4.4](#) to simulate the regular conditional distribution of  $X_0 \sim N(0, C)$  given  $\Pi^{\mathbb{S}}(X_0) = \bar{x}$ . In the following result  $\text{Gam}(a, b)$  denotes the Gamma distribution with shape parameter  $a > 0$  and inverse scale parameter  $b > 0$ .

**Proposition 4.5.** *Let  $\nu_0 = N(0, C)$  be given on  $\mathbb{R}^d$  and let  $\nu_{0|\Pi^{\mathbb{S}}}(\bar{x}, \cdot)$  denote the conditional distribution of  $X_0 \sim \nu_0$  given  $\Pi^{\mathbb{S}}(X_0) = \bar{x}$ . Then, for a non-negative real-valued random variable  $R$  satisfying  $R^2 \sim \text{Gam}(\frac{d}{2}, \frac{1}{2} \bar{x}^\top C^{-1} \bar{x})$  we have*

$$R\bar{x} \sim \nu_{0|\Pi^{\mathbb{S}}}(\bar{x}, \cdot).$$

**Proof.** We can write  $X_0 \sim \nu = N(0, C)$  as  $X_0 = R\bar{X}_0$ ,  $\bar{X}_0 := \Pi^{\mathbb{S}}(X_0)$ ,  $R := \|X_0\|$ . Thus, the condition of  $\Pi^{\mathbb{S}}(X_0) = \bar{x}$  yields the following conditional density of  $R$ :

$$f_{R|\Pi^{\mathbb{S}}(X_0)=\bar{x}}(r) \propto r^{d-1} \exp\left(-\frac{1}{2}(\bar{x}^\top C^{-1} \bar{x})r^2\right) = r^{d-1} \left(\exp\left(-\frac{1}{2}\bar{x}^\top C^{-1} \bar{x}\right)\right)^{r^2}.$$

By the change of variables  $r \mapsto r^2 =: r_2$  we get the following probability density for  $R^2$  given  $\Pi^{\mathbb{S}}(X_0) = \bar{x}$ :

$$f_{R^2|\Pi^{\mathbb{S}}(X_0)=\bar{x}}(r_2) \propto \frac{r_2^{(d-1)/2}}{2r_2^{1/2}} \left( e^{-\frac{1}{2}\bar{x}^\top C^{-1}\bar{x}} \right)^{r_2} \propto r_2^{d/2-1} e^{-(\frac{1}{2}\bar{x}^\top C^{-1}\bar{x})r_2}.$$

Thus,  $R^2$  conditioned on  $\Pi^{\mathbb{S}}(X_0) = \bar{x}$  follows the  $\text{Gam}(\frac{d}{2}, \frac{1}{2}\bar{x}^\top C^{-1}\bar{x})$ , as desired.  $\blacksquare$

**Resulting algorithms** We now provide two explicit algorithms for approximate sampling of target measures  $\mu$  on  $\mathbb{S}^{d-1}$  as given in (4.1). Algorithm 4 and Algorithm 5 result from applying the methodology of push-forward transition kernels to the pCN-MH algorithm and the ESS algorithm on  $\mathbb{H}$ , respectively. The pCN-MH algorithm and the ESS algorithm on  $\mathbb{H}$  were stated in Algorithm 1 and Algorithm 3.

---

**Algorithm 4.** Reprojected pCN-MH algorithm on  $\mathbb{S}^{d-1}$

---

- 1: **Given:** ACG prior  $\mu_0 = \text{ACG}(C)$  and target  $\mu$  as in (4.1)
  - 2: **Initial:** step size  $s \in (0, 1]$  and state  $\bar{x}_0 \in \mathbb{S}^{d-1}$
  - 3: **for**  $k \in \mathbb{N}_0$  **do**
  - 4: Draw a sample  $r_k^2$  of  $\text{Gam}(d/2, \frac{1}{2}\bar{x}_k^\top C^{-1}\bar{x}_k)$  and set  $x_k = r_k \bar{x}_k$
  - 5: Draw a sample  $w_k$  of  $\text{N}(0, C)$  and set  $y_{k+1} := \sqrt{1-s^2}x_k + sw_k$
  - 6: Set  $\bar{y}_{k+1} := y_{k+1}/\|y_{k+1}\|$
  - 7: Compute  $a := \min\{1, \exp(\bar{\Phi}(\bar{x}_k) - \bar{\Phi}(\bar{y}_{k+1}))\}$
  - 8: Draw a sample  $u$  of  $\text{U}[0, 1]$
  - 9: **if**  $u \leq a$  **then**
  - 10: Set  $\bar{x}_{k+1} = \bar{y}_{k+1}$
  - 11: **else**
  - 12: Set  $\bar{x}_{k+1} = \bar{x}_k$
  - 13: **end if**
  - 14: **end for**
- 

---

**Algorithm 5.** Reprojected ESS algorithm on  $\mathbb{S}^{d-1}$

---

- 1: **Given:** ACG prior  $\mu_0 = \text{ACG}(C)$  and target  $\mu$  as in (4.1)
  - 2: **Initial:** state  $\bar{x}_0 \in \mathbb{S}^{d-1}$
  - 3: **for**  $k \in \mathbb{N}_0$  **do**
  - 4: Draw a sample  $t \sim \text{U}[0, \exp(-\bar{\Phi}(\bar{x}_k))]$
  - 5: Draw a sample  $r_k^2$  of  $\text{Gam}(d/2, \frac{1}{2}\bar{x}_k^\top C^{-1}\bar{x}_k)$  and set  $x_k = r_k \bar{x}_k$
  - 6: Set  $x_{k+1} = \text{shrink-ellipse}(x_k, t)$  (see Algorithm 2)
  - 7: **end for**
- 

According to the third statement of Lemma 4.2, Algorithm 4 yields a MH algorithm on  $\mathbb{S}^{d-1}$ . Its acceptance probability is simply  $\bar{\alpha}(\bar{x}, \bar{y}) = \min\{1, \exp(\bar{\Phi}(\bar{y}) - \bar{\Phi}(\bar{x}))\}$ , for  $\bar{x}, \bar{y} \in \mathbb{S}^{d-1}$ , and its proposal kernel  $\bar{Q}: \mathbb{S}^{d-1} \times \mathcal{B}(\mathbb{S}^{d-1}) \rightarrow [0, 1]$  admits a proposal density  $\bar{q}: \mathbb{S}^{d-1} \times \mathbb{S}^{d-1} \rightarrow (0, \infty)$  with respect to the Hausdorff measure on  $\mathbb{S}^{d-1}$  given by

$$\bar{q}(\bar{x}, \bar{y}) = \int_0^\infty \int_0^\infty q(r\bar{x}, r'\bar{y}) f_{\bar{x}}(r) (r')^{d-1} dr dr' > 0, \quad \bar{x}, \bar{y} \in \mathbb{S}^{d-1}, \quad (4.10)$$

where  $q$  denotes the proposal density of the pCN proposal kernel  $Q(x, \cdot) = \text{N}(\sqrt{1-s^2}x, s^2C)$ ,  $x \in \mathbb{R}^d$ , and  $f_{\bar{x}}(r)$  denotes the conditional density of  $R = \|X\|$  for  $X \sim \text{N}(0, C)$  given  $\Pi^{\mathbb{S}}(X) = \bar{x}$ .



According to the proof of [Proposition 4.5](#), the density  $f_{\bar{x}}(r)$  takes the form

$$f_{\bar{x}}(r) := \frac{1}{c_{\bar{x}}} r^{d-1} \exp\left(-\frac{r^2}{2} \bar{x}^\top C^{-1} \bar{x}\right), \quad c_{\bar{x}} := \int_0^\infty r^{d-1} \exp\left(-\frac{r^2}{2} \bar{x}^\top C^{-1} \bar{x}\right) dr. \quad (4.11)$$

**Remark 4.6** (Interpretation of reprojected pCN proposal and reprojected ESS algorithm). An equivalent procedure for lines 4 to 6 in [Algorithm 4](#) is the following:

- 4: Draw a sample  $\bar{w}_k$  of  $\text{ACG}(C)$
- 5: Draw a sample  $r_k^2$  of  $\text{Gam}(d/2, \frac{1}{2} \bar{x}_k^\top C^{-1} \bar{x}_k)$  and a sample  $\mathbf{r}_k^2$  of  $\text{Gam}(d/2, \frac{1}{2} \bar{w}_k^\top C^{-1} \bar{w}_k)$
- 6: Set  $\bar{y}_{k+1} := \Pi^{\mathbb{S}}(\sqrt{1 - s^2} r_k \bar{x}_k + s \mathbf{r}_k \bar{w}_k)$

Thus, the proposal kernel of the reprojected pCN-MH algorithm samples a point  $\bar{y}$  on the arc between  $\bar{x}$  and  $\bar{w}$  on the sphere, where  $\bar{w}$  is a realisation of  $\bar{W} \sim \text{ACG}(C)$ . However, the “stepsize” — i.e. the angle  $\theta := \arccos(\langle \bar{y}, \bar{x} \rangle) \in [0, \arccos(\langle \bar{w}, \bar{x} \rangle)]$  between the proposed state  $\bar{y} \in \mathbb{S}^{d-1}$  and the current state  $\bar{x} \in \mathbb{S}^{d-1}$  — is random. In general, the distribution of the random stepsize depends on  $\bar{x}$  and  $\bar{w}$ .

Similarly, we can interpret the reprojected ESS algorithm as follows: Given a point  $\bar{x}_k \in \mathbb{S}^{d-1}$  we draw  $\bar{w}_k$  according to  $\text{ACG}(C)$  and consider the great circle  $\{\bar{y} = \cos(\theta) \bar{x} + \sin(\theta) \bar{w} \mid \theta \in [0, 2\pi)\}$ . The reprojected ESS algorithm then generates a new state  $\bar{x}_{k+1}$  belonging to the intersection of this great circle and the super-level set  $\{\bar{y} \in \mathbb{S}^{d-1} : \exp(-\bar{\Phi}(\bar{y})) \geq t\}$ , where  $t$  is drawn from  $U[0, \exp(-\bar{\Phi}(\bar{x}_k))]$ .

## 4.2. Uniform and geometric ergodicity

We investigate the exponential convergence behaviour of the transition kernels that correspond to the Markov chains that are realised either by [Algorithm 4](#) or [Algorithm 5](#). Since the underlying state space  $\mathbb{S}^{d-1}$  is compact, we aim for uniform ergodicity. The associated transition kernel  $\bar{K} : \mathbb{S}^{d-1} \times \mathcal{B}(\mathbb{S}^{d-1}) \rightarrow [0, 1]$  is said to be *uniformly ergodic*, if there are  $\kappa \in [0, 1)$  and  $c < \infty$  such that

$$\|\bar{K}^n(\bar{x}) - \mu\|_{\text{TV}} \leq c \kappa^{-n} \quad \forall \bar{x} \in \mathbb{S}^{d-1}. \quad (4.12)$$

It is well known, see, e.g. ([Douc et al., 2018](#), Theorem 15.3.1), that uniform ergodicity of a Markov chain is equivalent to the *smallness* of the whole state space. A set  $B \in \mathcal{B}(\mathbb{S}^{d-1})$  is called *small* with respect to a transition kernel  $\bar{K}$  if there exists some  $m \in \mathbb{N}$  and a nonzero measure  $\phi$  on  $(\mathbb{S}^{d-1}, \mathcal{B}(\mathbb{S}^{d-1}))$  such that

$$\bar{K}^m(\bar{x}, A) \geq \phi(A) \quad \forall A \in \mathcal{B}(\mathbb{S}^{d-1}), \bar{x} \in B. \quad (4.13)$$

By exploiting the particular structure [\(4.7\)](#) of push-forward transition kernels, we obtain the following result.

**Theorem 4.7.** *Let  $\bar{\Phi} : \mathbb{S}^{d-1} \rightarrow \mathbb{R}$  be uniformly bounded. Then, the transition kernels, which correspond to the Markov chains realised by [Algorithm 4](#) and [Algorithm 5](#), are uniformly ergodic.*

**Proof.** We first consider the reprojected pCN-MH kernel  $\bar{K}$ . Due to the boundedness of  $\bar{\Phi}$ , i.e.  $\underline{c} \leq \bar{\Phi}(\bar{x}) \leq \bar{c}$ , we have a lower bound on the acceptance probability

$$\bar{\alpha}(\bar{x}, \bar{y}) = \min\{1, \exp(\bar{\Phi}(\bar{y}) - \bar{\Phi}(\bar{x}))\} \geq \exp(\underline{c} - \bar{c}) > 0.$$

Hence, by the corresponding MH form of the reprojected pCN-MH kernel  $\bar{K}$  stated in [Lemma 4.2](#), we have for any  $A \in \mathcal{B}(\mathbb{S}^{d-1})$  and any  $\bar{x} \in \mathbb{S}^{d-1}$  that

$$\bar{K}(\bar{x}, A) \geq \int_A \bar{\alpha}(\bar{x}, \bar{y}) \bar{Q}(\bar{x}, d\bar{y}) \geq \exp(\underline{c} - \bar{c}) \bar{Q}(\bar{x}, A).$$

Recall that  $\bar{Q}$  possesses the density  $\bar{q}$  given in (4.10). Note that  $\bar{x} \mapsto \bar{x}^\top C^{-1} \bar{x}$  is bounded on  $\mathbb{S}^{d-1}$ , such that there exists for every  $r > 0$  a lower bound  $\underline{f}(r) > 0$  satisfying  $f_{\bar{x}}(r) \geq \underline{f}(r) > 0$  for every  $\bar{x} \in \mathbb{S}^{d-1}$ . Moreover, the density  $q(\cdot, y)$  of the pCN proposal kernel  $Q(x, \cdot) = \mathcal{N}(\sqrt{1-s^2}x, s^2C)$  is continuous. Therefore, it follows that  $q(x, y)$  is uniformly bounded away from zero for any  $x, y \in \mathbb{R}^d$  with  $\|x\|, \|y\| \leq 1$ . Hence, we can conclude that there exists some  $\epsilon > 0$  such that for every  $\bar{x}, \bar{y} \in \mathbb{S}^{d-1}$ ,  $\bar{q}(\bar{x}, \bar{y})$  in (4.10) satisfies  $\bar{q}(\bar{x}, \bar{y}) \geq \epsilon$ . This implies that  $\bar{Q}(\bar{x}, A) \geq \epsilon \mathcal{H}_{\mathbb{S}^{d-1}}(A)$ , for the Hausdorff measure  $\mathcal{H}_{\mathbb{S}^{d-1}}$  on  $\mathbb{S}^{d-1}$ . Thus,  $\mathbb{S}^{d-1}$  is small with respect to  $\bar{K}$  with  $\phi(A) := \exp(\underline{c} - \bar{c}) \epsilon \mathcal{H}_{\mathbb{S}^{d-1}}(A)$ .

Next, we consider the reprojected ESS kernel. Since  $\Phi$  on  $\mathbb{H} = \mathbb{R}^d$  is constructed from  $\bar{\Phi}$  on  $\mathbb{S}$  by (4.2), the boundedness of  $\bar{\Phi}$  implies the boundedness of  $\Phi$ . Hence, any compact set  $B \subset \mathbb{R}^d$  is small with respect to the ESS transition kernel  $K$ . The measure with respect to which the smallness property holds is  $\phi = \epsilon_B \lambda_B$ , where  $\epsilon_B > 0$  denotes a constant and  $\lambda_B$  is the Lebesgue measure restricted to the set  $B$ . This was recently shown in (Natarovskii et al., 2021a, Lemma 3.4). We now use this fact in order to show the smallness of  $\mathbb{S}^{d-1}$  with respect to the reprojected ESS transition kernel  $\bar{K}$ , for the measure  $\phi = \epsilon \mathcal{H}_{\mathbb{S}^{d-1}}$ . To this end, we apply the representation (4.7) with  $\mathbb{X} = \mathbb{R}^d$ ,  $\mathbb{Y} = \mathbb{S}^{d-1}$  and  $T = \Pi^{\mathbb{S}}$ :

$$\bar{K}(\bar{x}, A) = \int_0^\infty K(r\bar{x}, T^{-1}(A)) f_{\bar{x}}(r) dr$$

with  $f_{\bar{x}}$  as in (4.11). Again, since  $\bar{x} \mapsto \bar{x}^\top C^{-1} \bar{x}$  is bounded on  $\mathbb{S}^{d-1}$ , there exists for every  $r > 0$  a lower bound  $\underline{f}(r) > 0$  such that for every  $\bar{x} \in \mathbb{S}^{d-1}$ ,  $f_{\bar{x}}(r) \geq \underline{f}(r) > 0$ . Now fix  $B := B_1(0) = \{x \in \mathbb{R}^d \mid \|x\| \leq 1\}$  and note that  $B$  is small with respect to  $K$ . Thus

$$\bar{K}(\bar{x}, A) \geq \int_0^1 K(r\bar{x}, T^{-1}(A)) \underline{f}(r) dr \geq \epsilon_B \lambda_B(T^{-1}(A)) \int_0^1 \underline{f}(r) dr = \epsilon \mathcal{H}_{\mathbb{S}^{d-1}}(A)$$

where  $\epsilon := \epsilon_B \int_0^1 \underline{f}(r) dr \int_0^1 u^{d-1} du$ , since  $\lambda_B(T^{-1}(A)) = \int_A \int_0^1 u^{d-1} du \mathcal{H}_{\mathbb{S}^{d-1}}(d\bar{x})$ . ■

The boundedness assumption on  $\bar{\Phi}$  in Theorem 4.7 is rather mild and, for instance, satisfied if  $\bar{\Phi}: \mathbb{S}^{d-1} \rightarrow \mathbb{R}$  is continuous. For example, in the Bayesian level set inversion in Section 5 the corresponding  $\bar{\Phi}$  is bounded.

Theorem 4.7 yields uniform ergodicity in finite dimensions. However, we do not know how  $\kappa$  and  $c$  in (4.12) for Algorithm 4 and Algorithm 5 behave in the infinite-dimensional limit  $d \rightarrow \infty$ . The dimension depending convergence behaviour is discussed in the subsequent paragraph. There we consider geometric ergodicity as in (3.5) rather than uniform ergodicity as (4.12), because one can typically not expect uniform ergodicity or smallness of the state space to hold in the infinite-dimensional limit.

**Dimension-independent geometric ergodicity.** In order to study the geometric ergodicity of Markov chains generated by the reprojected pCN-MH and reprojected ESS algorithms, we can exploit Lemma 4.2. This lemma states that the spectral gaps of the reprojected transition kernels  $\bar{K}$  of Algorithm 4 and Algorithm 5 are at least as large as the spectral gaps of the transition kernels  $K$  of Algorithm 1 and Algorithm 3 respectively. In order to describe a dimension-independent spectral gap, we introduce the following notation: Given  $\mu_0 = \text{ACG}(C)$  with non-degenerate, trace-class covariance operator  $C: \mathbb{H} \rightarrow \mathbb{H}$  on an infinite-dimensional separable Hilbert space  $\mathbb{H}$ , let  $\{e_j \mid j \in \mathbb{N}\}$  be a complete orthonormal system in  $\mathbb{H}$  consisting of the eigenvectors of  $C$ . We now construct finite-dimensional approximations to the infinite-dimensional setting as follows: For  $d \in \mathbb{N}$ , let  $\mu_0^{(d)} = \text{ACG}(C_d)$  denote the ACG measure on

$\mathbb{S}^{d-1}$  resulting from the marginal of  $N(0, C)$  on  $\text{span}\{e_1, \dots, e_d\}$  and consider the target measure  $\mu^{(d)}$  on  $\mathbb{S}^{d-1}$  given by

$$\frac{d\mu^{(d)}}{d\mu_0^{(d)}}(\bar{x}) \propto \exp(-\bar{\Phi}(\bar{x})), \quad \bar{x} \in \mathbb{S}^{d-1}. \quad (4.14)$$

In order to apply  $\bar{\Phi}$  to  $\bar{x} \in \mathbb{S}^{d-1}$ , we view  $\mathbb{S}^{d-1}$  as the ‘‘equatorial’’ subsphere  $\{\bar{x}_1 e_1 + \dots + \bar{x}_d e_d \in \mathbb{H} : \bar{x} = (\bar{x}_1, \dots, \bar{x}_d) \in \mathbb{S}^{d-1}\}$  of  $\mathbb{S} \subset \mathbb{H}$ . Let

$$\frac{d\nu^{(d)}}{d\nu_0^{(d)}}(x) \propto \exp(-\Phi(x)), \quad x \in \mathbb{R}^d, \quad (4.15)$$

where  $\nu_0^{(d)} = N(0, C_d)$  and  $\Phi(x) := \bar{\Phi}(\Pi^{\mathbb{S}}(x))$  for  $x \in \mathbb{H}$ , as in (4.2). In order to apply  $\Phi$  to  $x \in \mathbb{R}^d$ , we view  $\mathbb{R}^d$  as the subspace  $\{x_1 e_1 + \dots + x_d e_d \in \mathbb{H} : x = (x_1, \dots, x_d) \in \mathbb{R}^d\}$  of  $\mathbb{H}$ .

For a reminder of the definition of  $\text{gap}_{\mu}(K)$  for a given measure  $\mu$  and transition kernel  $K$  we refer to (3.4). By Lemma 4.2 we obtain the following result.

**Corollary 4.8.** *Let  $\mu^{(d)}$  and  $\nu^{(d)}$  be as in (4.14) and (4.15) respectively. Let  $s \in (0, 1]$  and let  $K_s^{(d)}$  denote the pCN-MH transition kernel targeting  $\nu^{(d)}$  using the stepsize  $s$  in the proposal. If there exists a  $\beta > 0$  such that*

$$\inf_{d \in \mathbb{N}} \text{gap}_{\nu^{(d)}}(K_s^{(d)}) \geq \beta \quad (4.16)$$

*then the rejected pCN-MH transition kernel  $\bar{K}_s^{(d)} := (\Pi^{\mathbb{S}})_{\#} K_s^{(d)}$  targeting  $\mu^{(d)}$  on  $\mathbb{S}^{d-1}$  satisfies*

$$\inf_{d \in \mathbb{N}} \text{gap}_{\mu^{(d)}}(\bar{K}_s^{(d)}) \geq \beta. \quad (4.17)$$

*The same statement holds for the rejected ESS transition kernel  $\bar{K}^{(d)} := (\Pi^{\mathbb{S}})_{\#} K^{(d)}$ .*

Dimension independence of the spectral gap of the ESS transition kernel has been demonstrated in the literature by numerical experiments (Natarovskii et al., 2021a). However, to the best of our knowledge, no theoretical proof is available. Therefore, we focus on the pCN-MH algorithm, for which (4.16) was shown by Hairer et al. (2014) under certain assumptions on  $\bar{\Phi}$ . For convenience, we summarise their result:

**Theorem 4.9.** *Let  $s \in (0, 1]$  and let  $K_s^{(d)}$  denote the pCN-MH transition kernel targeting  $\nu^{(d)}$  using the stepsize  $s$  in the proposal. Suppose the following conditions hold:*

(a) *There exist some  $R > 0$  and  $\underline{\alpha} \in \mathbb{R}$  such that for all  $x \in \mathbb{H}$  with  $\|x\| > R$  we have*

$$\Phi(y) < \Phi(x) - \underline{\alpha} \quad \forall y \in \mathbb{H}: \|y - \sqrt{1 - s^2}x\| \leq \frac{1}{2}(1 - \sqrt{1 - s^2})\|x\|.$$

(b) *The function  $e^{-\Phi}$  is integrable with respect to  $\nu_0 = N(0, C)$ .*

(c) *For every  $\gamma > 0$  there exists some  $C_{\gamma} < \infty$  such that*

$$|\Phi(x) - \Phi(y)| \leq C_{\gamma} e^{\gamma r} \quad \forall x, y \in \mathbb{H}: \|x\|, \|y\| \leq r.$$

*Then there exists a  $\beta > 0$  such that (4.16) holds.*

In order to discuss and partially verify the assumptions of the former theorem for  $\Phi = \bar{\Phi} \circ \Pi^{\mathbb{S}}$ , we state the following result.

**Proposition 4.10.** *Let  $\bar{\Phi}: \mathbb{S} \rightarrow \mathbb{R}$  be uniformly bounded. Then,  $\Phi = \bar{\Phi} \circ \Pi^{\mathbb{S}}$  satisfies conditions (a) and (b) of Theorem 4.9.*

**Proof.** Condition (b) in [Theorem 4.9](#) is satisfied, since  $\bar{\Phi}$  is bounded. Hence  $\Phi = \bar{\Phi} \circ \Pi^{\mathbb{S}}$  is bounded. Boundedness of  $\Phi$ , e.g. according to  $\underline{c} \leq \bar{\Phi}(\bar{x}) \leq \bar{c}$ , implies

$$\Phi(y) < \Phi(x) - (\underline{c} - \bar{c} - 1)$$

for any  $x, y \in \mathbb{H}$ . Thus, Condition (a) of [Theorem 4.9](#) is satisfied, with  $\underline{\alpha} = \underline{c} - \bar{c} - 1 < 0$  and arbitrary  $R > 0$ , for example.  $\blacksquare$

Unfortunately, the function  $\Phi = \bar{\Phi} \circ \Pi^{\mathbb{S}}$  does not satisfy Condition (c) of [Theorem 4.9](#), because  $\Phi$  is discontinuous at  $x = 0$  whenever  $\bar{\Phi}$  is non-constant. However, we believe that the third condition in [Theorem 4.9](#) could be weakened to the case where  $\Phi$  is locally Lipschitz continuous outside of a sufficiently small ball  $B_r(0) \subset \mathbb{H}$ . This can be justified by the intuition that a bounded perturbation of  $\Phi$  in a sufficiently small neighbourhood of 0 should have little effect on the geometric ergodicity of the pCN-MH algorithm. We leave a rigorous mathematical discussion of this point for future research. In addition, we note that the numerical results in [Section 5](#) suggest that (4.17) holds for bounded  $\bar{\Phi}$ . See for example [Figure 5.4](#), which shows that the performance of the reprojected pCN and reprojected ESS algorithms does not deteriorate as the dimension increases. This numerical evidence suggests that a dimension-independent spectral gap exists.

### 4.3. Related approaches and their shortcomings

Given a Markov chain  $(X_n)_{n \in \mathbb{N}}$  with  $\nu$ -reversible transition kernel  $K$ , one can also consider  $(T(X_n))_{n \in \mathbb{N}}$  as a sequence of random variables on  $\mathbb{Y}$ . In our prototypical setting where  $\mathbb{Y} = \mathbb{S}$ , the stochastic process  $(T(X_n))_{n \in \mathbb{N}}$  is simply the projection of the Markov chain  $(X_n)_{n \in \mathbb{N}}$  onto  $\mathbb{S}$  via  $T = \Pi^{\mathbb{S}}$ . Hence, one can think of this as a simple projection approach. If the law  $\mathcal{L}(X_n)$  of  $X_n$  converges to  $\nu$  in the total variation norm as  $n \rightarrow \infty$ , then the law  $\mathcal{L}(T(X_n))$  of  $T(X_n)$  will also converge to  $T_{\sharp}\nu$  in the total variation norm, since

$$\|\mathcal{L}(T(X_n)) - T_{\sharp}\nu\|_{\text{TV}} \leq \|\mathcal{L}(X_n) - \nu\|_{\text{TV}}$$

due to

$$\|T_{\sharp}\rho - T_{\sharp}\nu\|_{\text{TV}} = \sup_{A \in \mathcal{B}(\mathbb{S})} |\rho(T^{-1}(A)) - \nu(T^{-1}(A))| = \sup_{A \in \sigma(T)} |\rho(A) - \nu(A)| \leq \|\rho - \nu\|_{\text{TV}}$$

with  $\mathcal{L}(T(X_n)) = T_{\sharp}\rho$  and  $\mathcal{L}(X_n) = \rho$ , where  $\sigma(T)$  denotes the Borel  $\sigma$ -algebra generated by  $T$ . However, the sequence  $(T(X_n))_{n \in \mathbb{N}}$  fails, in general, to be a Markov chain, see, e.g. ([Glover and Mitro, 1990](#)) and the references therein. In particular, we provide an explicit counterexample in case of  $T = \Pi^{\mathbb{S}}$  in [Appendix B](#). We mention the result ([Rosenblatt, 1966](#), Theorem 3), which considers general Markov processes  $(X_i)_{i \in I}$  that may be discrete or continuous in time or space, and specifies sufficient and necessary conditions on a measurable mapping  $T$  such that  $(T(X_i))_{i \in I}$  is again a Markov process.

Another related approach can be constructed as follows. Recall that in (4.7) we average with respect to the regular conditional distribution given  $T(x) = \bar{x}$ , i.e.  $\nu_T(\bar{x}, \cdot)$ . It is natural to ask if this averaging is necessary. For instance, one could simply define the transition kernel

$$\bar{K}(\bar{x}, A) := K(\bar{x}, (\Pi^{\mathbb{S}})^{-1}(A)) \quad \forall \bar{x} \in \mathbb{Y}, A \in \mathcal{B}(\mathbb{Y}). \quad (4.18)$$

We shall refer to the transition kernel  $\bar{K}$  in (4.18) as the ‘naïve reprojected kernel’. In the setting where the topological spaces  $\mathbb{X}$  and  $\mathbb{Y}$  satisfy  $\mathbb{Y} \subset \mathbb{X}$ , one realises  $\bar{y}$  with respect to  $\bar{K}(\bar{x}, \cdot)$  by first choosing  $y$  according to  $K(\bar{x}, \cdot)$  and then setting  $\bar{y} := T(y)$ , as illustrated in

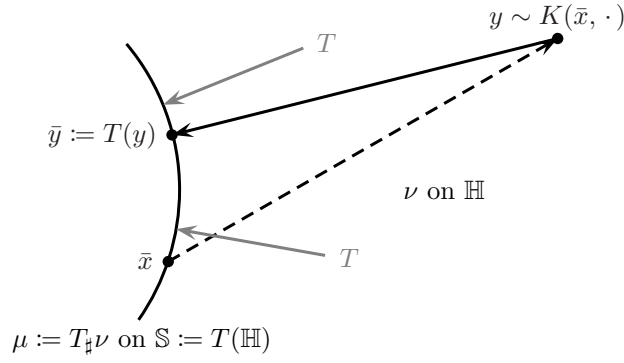


**Figure 4.2.:** Illustration of the steps for drawing states using the naïve reprojected kernel  $\bar{K}$  in (4.18) for  $\mathbb{X} = \mathbb{H}$ ,  $\mathbb{Y} = \mathbb{S}$ , and  $T = \Pi^{\mathbb{S}}$  in (2.8). Starting from  $\bar{x}$ , an intermediate state  $y \in \mathbb{H}$  is drawn from the  $\nu$ -reversible transition kernel  $K(\bar{x}, \cdot)$  on  $\mathbb{H}$ . The next state drawn from the naïve reprojected kernel  $\bar{K}(\bar{x}, \cdot)$  is then  $\bar{y} := T(y) = \Pi^{\mathbb{S}}(y)$ . Solid arrows indicate deterministic maps, whereas dashed arrows indicate randomised maps, i.e. draws from transition kernels.

Figure 4.2. That is, one first transitions from  $\bar{x} \in \mathbb{Y}$  to a state  $y$  in the ambient space  $\mathbb{X}$ , and then “reprojects” this state  $y$  into  $\bar{y} \in \mathbb{Y}$  using the mapping  $T$ .

Unlike the projection approach described earlier, this method yields a Markov chain. However, as numerical experiments show, the naïve reprojected kernel  $\bar{K}$  does not have  $\mu$  as its stationary distribution, even if  $K$  is  $\nu$ -invariant or  $\nu$ -reversible. To see why, recall that  $\mu = T_{\#}\nu$ . Hence,  $\bar{K}$  is  $\mu$ -invariant if and only if

$$\int_{\mathbb{Y}} \bar{K}(\bar{x}, A) \mu(d\bar{x}) = \int_{\mathbb{Y}} K(\bar{x}, T^{-1}(A)) \mu(d\bar{x}) = \int_{\mathbb{X}} K(T(x), T^{-1}(A)) \nu(dx) = \nu(T^{-1}(A))$$

for all  $A \in \mathcal{B}(\mathbb{Y})$ . If  $K$  is  $\nu$ -invariant, then by definition  $\nu(T^{-1}(A)) = \int_{\mathbb{X}} K(x, T^{-1}(A)) \nu(dx)$ . This yields the following necessary and sufficient condition for the  $\mu$ -invariance of  $\bar{K}$ :

$$\int_{\mathbb{X}} K(x, T^{-1}(A)) \nu(dx) = \int_{\mathbb{X}} K(T(x), T^{-1}(A)) \nu(dx), \quad \forall A \in \mathcal{B}(\mathbb{Y}).$$

Based upon numerical experiments, we argue that this condition is not necessarily satisfied in the setting where  $\mathbb{X} = \mathbb{H}$ ,  $\mathbb{Y} = \mathbb{S}$ , and  $T = \Pi^{\mathbb{S}}$ . Let  $\mathbb{H} = \mathbb{R}^3$ ,  $\nu = \mathcal{N}(0, C)$  with covariance matrix  $C \in \mathbb{R}^{3 \times 3}$ , and consider the  $\nu$ -reversible pCN proposal kernel

$$K(x) = \mathcal{N}(\sqrt{1-s^2}x, s^2C), \quad \text{with } s = 0.7 \text{ and } C = \begin{pmatrix} 1.25 & 0.33 & -1.62 \\ 0.33 & 0.42 & -0.09 \\ -1.62 & -0.09 & 2.85 \end{pmatrix}.$$

We now estimate and compare the probability density function of the marginals of  $\mu = \Pi_{\#}^{\mathbb{S}}\nu$  and  $\mu\bar{K}$  by kernel density estimation based on  $10^6$  independent samples of  $\mu$  and  $\mu\bar{K}$ , respectively.<sup>3</sup> The results are displayed in Figure 4.3. The important observation is that the marginals of  $\mu$  (dashed yellow line) and  $\mu\bar{K}$  (dotted blue line) differ. Hence,  $\bar{K}$  is not  $\mu$ -invariant in this case. Note that the marginals of  $\mu$  (dashed yellow line) coincide with the marginals of  $\mu(\Pi_{\#}^{\mathbb{S}}K)$  (solid red line), where  $\Pi_{\#}^{\mathbb{S}}K$  is the  $\mu$ -reversible transition kernel of the reprojected Markov chain using the push-forward transition kernel  $T_{\#}K$  in (4.5).

<sup>3</sup>The samples were generated as follows: 1) Draw a sample  $x$  from  $\nu$  and set  $\bar{x} := \Pi^{\mathbb{S}}(x)$ , so that  $\bar{x}$  is a sample draw from  $\mu$ ; 2) draw another sample  $w$  from  $\nu$  and set  $y := \sqrt{1-s^2}\bar{x} + sw$ , so that  $\bar{y} = \Pi^{\mathbb{S}}(y)$  is a sample draw from  $\mu\bar{K}$ .

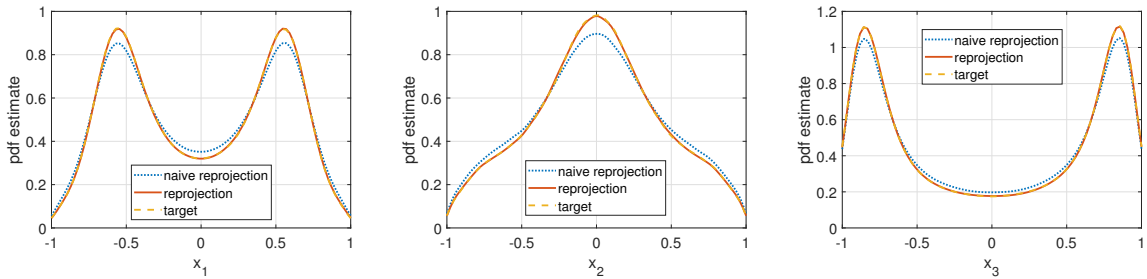


**Figure 4.3.:** Comparison of marginals of  $\mu = \Pi_{\sharp}^{\mathbb{S}}\nu$  (target),  $\mu_{\bar{K}}$  (naïve reprojection) with  $\bar{K}$  as in (4.18), and  $\mu(\Pi_{\sharp}^{\mathbb{S}}K)$  (reprojection) with  $\Pi_{\sharp}^{\mathbb{S}}K$  as in (4.7) with pCN-kernel  $K$  and  $T = \Pi^{\mathbb{S}}$ .

#### 4.4. Existing random walk-like MCMC algorithms on $\mathbb{S}^{d-1}$

We describe now two MH algorithms from the literature. These algorithms use random walk-like proposals that are defined on general, finite-dimensional manifolds  $\mathbb{M}$ . We shall compare the algorithms described in Section 4.1 with these algorithms on a numerical example in Section 5. In the following paragraphs we first describe the corresponding MH algorithm for a general manifold  $\mathbb{M}$  and then provide the particular algorithm for the case of sampling on a sphere  $\mathbb{M} = \mathbb{S}^{d-1}$ . Throughout, we assume that  $\mathbb{M}$  admits a Hausdorff measure  $\mathcal{H}_{\mathbb{M}}$  and that the target probability measure  $\mu$  on  $\mathbb{M}$  is given by an unnormalised density  $\rho$  with respect to  $\mathcal{H}_{\mathbb{M}}$ , that is,

$$\frac{d\mu}{d\mathcal{H}_{\mathbb{M}}}(\bar{x}) \propto \rho(\bar{x}), \quad \bar{x} \in \mathbb{M}. \quad (4.19)$$

When  $\mathbb{M} = \mathbb{S}^{d-1}$  and  $\mu$  is a posterior measure with respect to an ACG prior  $\mu_0 = \text{ACG}(C)$  as in (4.1), we have

$$\rho(\bar{x}) = \frac{\exp(-\bar{\Phi}(\bar{x}))}{\|\bar{x}\|_C^d}.$$

**Geodesic random walk MH algorithm.** Assume that  $\mathcal{H}_{\mathbb{M}}(\mathbb{M}) < \infty$ . Then the uniform measure  $U(\mathbb{M})$  on  $\mathbb{M}$  is defined via  $U(\mathbb{M})(A) := \mathcal{H}_{\mathbb{M}}(A)/\mathcal{H}_{\mathbb{M}}(\mathbb{M})$  for  $A \in \mathcal{B}(\mathbb{M})$ . The geodesic random walk as described in (Mangoubi and Smith, 2018) yields a Markov chain  $(\bar{X}_k)_{k \in \mathbb{N}}$  on  $\mathbb{M}$  with  $U(\mathbb{M})$  as its limit distribution. For any  $\bar{x} \in \mathbb{M}$ , denote the tangent space at  $\bar{x}$  by  $\mathcal{T}_{\bar{x}}\mathbb{M}$ , and for any vector  $v \in \mathcal{T}_{\bar{x}}\mathbb{M}$ , denote by  $\gamma_{\bar{x},v}$  the unique geodesic  $\gamma_{\bar{x},v}: [0, \infty) \rightarrow \mathbb{M}$  on  $\mathbb{M}$  that satisfies  $\gamma_{\bar{x},v}(0) = \bar{x}$  and  $\gamma'_{\bar{x},v}(0) = v$ , where  $\gamma'$  denotes the first derivative.

Next, we present how a transition from a state  $\bar{x}$  to a state  $\bar{y}$  proceeds in the geodesic random walk algorithm.

**Transition mechanism 4.11 (Geodesic random walk).** Given the current state  $\bar{x} \in \mathbb{M}$  one obtains the next state  $\bar{y} \in \mathbb{M}$  for fixed  $t > 0$  as follows:

- (1) Draw from the uniform distribution on the unit sphere in  $\mathcal{T}_{\bar{x}}\mathbb{M}$  and call the result  $v$ ;
- (2) Set  $\bar{y} = \gamma_{\bar{x},v}(t)$ .

Hence, in order to sample approximately from  $\mu$  as in (4.19), we can employ the geodesic random walk kernel as a proposal kernel in a MH algorithm. The resulting acceptance probability  $\alpha$  involves ratios of the unnormalised density  $\rho$  in (4.19). For  $\mathbb{M} = \mathbb{S}^{d-1}$ , numerical experiments indicate that the corresponding geodesic random walk transition kernel is reversible with respect to  $U(\mathbb{S}^{d-1})$ . Therefore, the resulting algorithm for realising the Metropolised geodesic random walk is as given in Algorithm 6.

**Remark 4.12.** In order to sample from the uniform distribution on the unit sphere in  $\mathcal{T}_{\bar{x}}\mathbb{M}$  we can use the tools outlined by [Zappa et al. \(2018\)](#) for the case of constrained  $m$ -dimensional manifolds embedded into  $\mathbb{R}^d$ ,  $d > m$ , via

$$\mathbb{M} = \left\{ x \in \mathbb{R}^d \mid q_i(x) = 0 \quad \forall i = 1, \dots, L \right\}, \quad L \geq d - m, \quad (4.20)$$

where  $q_i: \mathbb{R} \rightarrow \mathbb{R}$  are smooth functions. In particular, an orthonormal basis (ONB) of  $\mathcal{T}_{\bar{x}}\mathbb{M}$  can be obtained by a QR decomposition of the Jacobian of  $Q(x) := (q_1(x), \dots, q_L(x))$  evaluated at  $x = \bar{x}$ . Let us denote such a basis by  $u_1, \dots, u_m \in \mathbb{R}^d$  and store the vectors in the columns of  $U_{\bar{x}} = [u_1 \mid \dots \mid u_m] \in \mathbb{R}^{d \times m}$ . Drawing a sample  $w$  from  $U(\mathbb{S}^{m-1})$  and setting  $v = U_{\bar{x}}w$  yields a sample according to the uniform distribution on the sphere in  $\mathcal{T}_{\bar{x}}\mathbb{M}$ . If  $\mathbb{M} = \mathbb{S}^{d-1}$ , then we have only one constraint function, i.e.  $q_1(x) = \|x\|^2 - 1$ . Hence, the tangent space  $\mathcal{T}_{\bar{x}}\mathbb{M}$  coincides with the orthogonal complement  $\bar{x}^\perp$  of  $\text{span}\{\bar{x}\}$ .

---

**Algorithm 6.** Geodesic random walk-MH on  $\mathbb{S}^{d-1}$  ([Mangoubi and Smith, 2018](#))

---

```

1: Given: time  $t \in (0, \frac{\pi}{2}]$  and initial state  $\bar{x}_0 \in \mathbb{S}^{d-1}$ 
2: for  $k \in \mathbb{N}_0$  do
3:   Compute ONB matrix  $U_{\bar{x}_k} \in \mathbb{R}^{d \times (d-1)}$  of  $\bar{x}_k^\perp$  according to Remark 4.12
4:   Draw a sample  $w_k$  from  $U(\mathbb{S}^{d-2})$  and set  $v_k := U_{\bar{x}_k}w_k$ 
5:   Set  $\bar{y}_{k+1} := \cos(t)\bar{x}_k + \sin(t)v_k$ 
6:   Compute  $a := \min\{1, \rho(\bar{y}_{k+1})/\rho(\bar{x}_k)\}$ 
7:   Draw a sample  $u$  from  $U([0, 1])$ 
8:   if  $u \leq a$  then
9:     Set  $\bar{x}_{k+1} = \bar{y}_{k+1}$ 
10:  else
11:    Set  $\bar{x}_{k+1} = \bar{x}_k$ 
12:  end if
13: end for

```

---

**Remark 4.13** (Ergodicity). In ([Mangoubi and Smith, 2018](#), Theorem 7.1) it is shown that the geodesic random walk, i.e. the proposal kernel of [Algorithm 6](#), possesses a mixing time with respect to a Wasserstein distance that depends only on the positive curvature of the manifold  $\mathbb{M}$ , given a suitably small integration time  $t$ . Thus, in case of the sphere  $\mathbb{M} = \mathbb{S}^{d-1}$ , the mixing time is independent of the dimension  $d$  for any  $t \in (0, \frac{\pi}{2}]$ . However, this statement solely holds for the proposal chain. As we will see in [Section 5](#), the MH algorithm based on the geodesic random walk proposal shows deteriorating efficiency as  $d \rightarrow \infty$ . Besides that, also the uniform ergodicity of [Algorithm 6](#), or the geodesic random walk itself, is not obvious and left open for future research.

**MH algorithm by [Zappa et al. \(2018\)](#)** The MH algorithm presented in ([Zappa et al., 2018](#)) shows some similarities with our method, in the sense that it first proposes a new state in the ambient Euclidean space which is then projected to the manifold  $\mathbb{M}$ . The manifold  $\mathbb{M}$  is assumed to be of the form (4.20). Given a current state  $\bar{x} \in \mathbb{M}$ , we first draw a tangent vector  $v \in \mathcal{T}_{\bar{x}}\mathbb{M}$ , but this time with respect to an isotropic multivariate Gaussian measure  $N(0, s^2 I_{d-m})$ . Here, we can employ again the technique explained in [Remark 4.12](#), by using an ONB matrix  $U_{\bar{x}} \in \mathbb{R}^{d \times (d-m)}$  of  $\mathcal{T}_{\bar{x}}\mathbb{M}$ , drawing  $w$  from  $N(0, s^2 I_{d-m})$ , and defining the resulting sample  $v = U_{\bar{x}}w$ . We then consider  $x := \bar{x} + v \in \mathbb{R}^d$ , and project  $x$  to some  $\bar{y} \in \mathbb{M}$  by

$$\bar{y} := x + w \quad \text{with suitable} \quad w \in (\mathcal{T}_{\bar{x}}\mathbb{M})^\perp.$$

In general, computing  $w$  and  $\bar{y}$  requires solving a nonlinear system; see (Zappa et al., 2018, Equation (2.5)). For  $\mathbb{M} = \mathbb{S}^{d-1}$  the situation is rather easy: Since  $(\mathcal{T}_{\bar{x}}\mathbb{M})^\perp = \text{span}\{\bar{x}\}$ , we have  $w = a\bar{x}$  with  $a \in \mathbb{R}$  satisfying  $\|\bar{y}\| = \|(1+a)\bar{x} + v\| = 1$ . Since  $\bar{x} \perp v$ , if  $\|v\|^2 \leq 1$ , then

$$\bar{y} = \sqrt{1 - \|v\|^2}\bar{x} + v.$$

If  $\|v\|^2 > 1$ , then  $x$  cannot be projected back to the sphere along  $\text{span}\{\bar{x}\}$ . In this case,  $x$  is rejected and the Markov chain remains at its current state, i.e. in the  $k$ th iteration it is realised as  $\bar{x}_{k+1} = \bar{x}_k$ . In case of a successful proposal  $\bar{y}$  we still require a Metropolis step, where the correct acceptance probability for  $\bar{y}$  also requires the ingredients of the reverse move from  $\bar{y}$  to  $\bar{x}$ . That is, we require  $\tilde{v} \in \mathcal{T}_{\bar{y}}\mathbb{M}$  such that

$$\bar{x} = \bar{y} + \tilde{v} + \tilde{w}, \quad \tilde{w} \in (\mathcal{T}_{\bar{y}}\mathbb{M})^\perp.$$

The acceptance probability in the MH algorithm targeting  $\mu$  as in (4.19) is then given by

$$\alpha(\bar{x}, \bar{y}) = \min\left\{1, \frac{\rho(\bar{y})p(\bar{y}, \tilde{v})}{\rho(\bar{x})p(\bar{x}, v)}\right\},$$

where  $p(\bar{y}, \tilde{v}) \propto \exp\left(-\frac{\|U_{\bar{y}}^\top \tilde{v}\|^2}{2s^2}\right)$  denotes the proposal density for the tangential moves. Since  $U_{\bar{y}}$  is orthonormal, we have  $\|U_{\bar{y}}^\top \tilde{v}\| = \|\tilde{v}\|$ . Moreover, for  $\mathbb{M} = \mathbb{S}^{d-1}$ , the vector  $\tilde{v} \in \mathcal{T}_{\bar{y}}\mathbb{M}$  for going from  $\bar{y} = \sqrt{1 - \|v\|^2}\bar{x} + v$  back to  $\bar{x}$  can be computed easily by projecting  $\bar{x} - \bar{y}$  onto  $\mathcal{T}_{\bar{y}}\mathbb{M} = (\bar{y})^\perp$ , which yields

$$\tilde{v} = \bar{x} - \bar{y} - \langle \bar{x} - \bar{y}, \bar{y} \rangle \bar{y} = \|v\|^2 \bar{x} - \sqrt{1 - \|v\|^2} v.$$

In particular, since  $\bar{x} \perp v$ , we obtain that  $\|\tilde{v}\| = \|v\|$ . Hence, for  $\mathbb{M} = \mathbb{S}^{d-1}$  the acceptance probability is just  $\alpha(\bar{x}, \bar{y}) = \min\{1, \rho(\bar{y})/\rho(\bar{x})\}$ . We summarise the resulting MH algorithm in Algorithm 7.

---

**Algorithm 7.** MH algorithm on  $\mathbb{S}^{d-1}$  (Zappa et al., 2018)

---

- 1: **Given:** step size  $s > 0$  and initial state  $\bar{x}_0 \in \mathbb{S}^{d-1}$
  - 2: **for**  $k \in \mathbb{N}_0$  **do**
  - 3:   Compute ONB matrix  $U_{\bar{x}_k} \in \mathbb{R}^{d \times (d-1)}$  of  $\bar{x}_k^\perp$  according to Remark 4.12
  - 4:   Draw a sample  $w_k$  of  $\mathcal{N}(0, s^2 I_{d-1})$  and set  $v_k := U_{\bar{x}_k} w_k$
  - 5:   **if**  $\|v_k\| > 1$  **then**
  - 6:     Set  $\bar{x}_{k+1} = \bar{x}_k$
  - 7:   **else**
  - 8:     Set  $\bar{y}_{k+1} := \sqrt{1 - \|v_k\|^2} \bar{x}_k + v_k$
  - 9:     Compute  $a := \min\{1, \rho(\bar{y}_{k+1})/\rho(\bar{x}_k)\}$
  - 10:    Draw a sample  $u$  of  $\mathcal{U}[0, 1]$
  - 11:    **if**  $u \leq a$  **then**
  - 12:     Set  $\bar{x}_{k+1} = \bar{y}_{k+1}$
  - 13:    **else**
  - 14:     Set  $\bar{x}_{k+1} = \bar{x}_k$
  - 15:    **end if**
  - 16:   **end if**
  - 17: **end for**
-



**Remark 4.14** (Ergodicity). As stated in (Zappa et al., 2018, Section 2.1), their proposed MH algorithm yields uniform ergodicity for compact  $\mathbb{M}$  and continuous  $\rho$ . This follows by standard arguments for MH algorithms with continuous proposal densities bounded away from zero on compact state spaces, see, e.g. (Douc et al., 2018, Example 15.3.2). In particular, Algorithm 7 yields uniformly ergodic Markov chains under the conditions of Theorem 4.7.

## 5. Numerical illustrations

We now demonstrate the dimension-independent performance of the reprojected pCN-MH algorithm and the reprojected ESS algorithm for Bayesian binary classification. We first describe the general setting of level set inversion following (Iglesias et al., 2016) and then consider a specific example. We will use the specific example to illustrate the dimension-dependent performance of the geodesic random walk MH algorithm of Mangoubi and Smith (2018) and the MH algorithm of Zappa et al. (2018).

### 5.1. Level set inversion

For simplicity, we focus on the single-phase Darcy flow model or groundwater flow problem on a bounded domain  $D \subset \mathbb{R}^2$ . This problem is described by the elliptic partial differential equation (PDE)

$$-\nabla(e^u \nabla p) = f \text{ in } D, \quad (5.1a)$$

$$p = \kappa \text{ on } \partial D, \quad (5.1b)$$

where  $p$  denotes a fluid pressure field,  $f$  describes sources and sinks, and  $u$  is the log-permeability parameter. Let  $\mathcal{U} := L^\infty(D)$  and  $\mathcal{V} := \{\tilde{p} \in H^1(D) \mid \tilde{p} = \kappa \text{ on } \partial D\}$ . If  $u \in \mathcal{U}$ , then  $e^u \in L^\infty(D)$ , and given suitable boundary data  $\kappa$  and  $f \in L^2(D)$ , a unique weak solution  $p \in \mathcal{V}$  of (5.1) exists. Denote the solution map that maps the log-permeability  $u$  to the corresponding solution  $p$  by  $G: \mathcal{U} \rightarrow \mathcal{V}$ . Then  $G$  is locally Lipschitz continuous, see, e.g. (Bonito et al., 2017). The goal is to infer the log-permeability  $u$  based on noisy observations of the form

$$y = O \circ G(u) + \eta, \quad (5.2)$$

where  $O: \mathcal{V} \rightarrow \mathbb{R}^J$  denotes for some  $J \in \mathbb{N}$  a bounded linear observation operator and  $\eta$  describes observational noise. We assume that  $\eta \sim \mathcal{N}(0, \Sigma)$  with known covariance  $\Sigma \in \mathbb{R}^{J \times J}$ .

In level set inversion we assume that the domain  $D$  is divided into disjoint regions  $D_i \subset D$ ,  $i = 1, \dots, n$ , i.e. the closure  $\overline{D}$  of  $D$  is the union of the closures of the  $D_i$ . The subdomains  $D_i$  describe the location of different materials with different constant log-permeabilities  $u_i \in \mathbb{R}$ . In particular, in level set inversion we assume that  $u$  takes the form

$$u(t) = \sum_{i=1}^n u_i \mathbb{1}_{D_i}(t), \quad t \in D,$$

where  $\mathbb{1}_{D_i}$  denotes the indicator function of  $D_i$  and where the values  $u_i$  are known a-priori. We then infer the location of specific regions  $D_i$  based on the noisy data  $y \in \mathbb{R}^J$  given by (5.2). To this end, we introduce a so-called *level set function*  $g \in C(\overline{D})$ , a vector  $\gamma = (\gamma_1, \dots, \gamma_{n-1}) \in \mathbb{R}^{n-1}$  of strictly increasing numbers, as well as the *level set map*  $\mathcal{L}: C(\overline{D}) \rightarrow \mathcal{U}$  defined by

$$g \mapsto \mathcal{L}(g) := \sum_{i=1}^n u_i \mathbb{1}_{D_i(g)}, \quad D_i(g) := \{t \in D \mid \gamma_{i-1} \leq g(t) < \gamma_i\}, \quad i = 1, \dots, n, \quad (5.3)$$

with  $\gamma_0 := -\infty$  and  $\gamma_n := \infty$ . Fix the vector  $\gamma$  of thresholds. The level set inverse problem consists in inferring a suitable level set function  $g \in C(\bar{D})$  that describes the decomposition of  $D$  into subregions  $D_i$ , given the noisy observations  $y = O \circ G \circ \mathcal{L}(g) + \eta$  in (5.2).

In the following, we focus on the case of *binary classification*, i.e.  $n = 2$  subregions  $D_1$  and  $D_2$ . These subregions model background material and abnormal material, for instance. Here, without loss of generality we may assume that  $\gamma_1 = 0$ , so that

$$D_1(g) = \{t \in D \mid g(t) < 0\}, \quad D_2(g) = \{t \in D \mid g(t) \geq 0\}.$$

Hence,  $\mathcal{L}(\alpha g) = \mathcal{L}(g)$  for any  $\alpha > 0$ . This expresses the invariance property of the level set map  $\mathcal{L}$  under radial projection, i.e. that  $\mathcal{L} = \mathcal{L} \circ \Pi^{\mathbb{S}}$  for  $\Pi^{\mathbb{S}}$  defined in (2.8). This invariance property means that in binary classification, one only needs to infer the ‘direction’ of the level set function  $g \in C(\bar{D})$ . In particular, the binary classification problem is naturally posed on the unit sphere  $\mathbb{S}$  in the Banach space  $C(\bar{D})$ .

Next, we explain the Bayesian approach to level set inversion, which yields an inverse problem on the unit sphere in a suitable Hilbert space  $\mathbb{H}$ .

**Bayesian level set inversion.** For the inverse problem of inferring the level set function  $g \in C(\bar{D})$ , one often uses a Gaussian prior, in form of a pathwise continuous Gaussian process model for  $g$  with corresponding continuous pointwise mean function  $m(t) = \mathbb{E}[g(t)]$  and continuous pointwise covariance function  $c(s, t) := \text{Cov}[g(s), g(t)]$  (Iglesias et al., 2016; Dunlop et al., 2017). Usually  $m$  is set to  $m \equiv 0$  and for  $c(\cdot, \cdot)$  a Whittle–Matérn covariance function is chosen. By the natural embedding of  $C(\bar{D})$  into  $L^2(D)$ , we can view  $g$  then also as a Gaussian random variable in the Hilbert space  $L^2(D)$  taking values in  $C(\bar{D}) \subseteq L^2(D)$  almost surely. Denote the corresponding distribution of  $g$  in  $L^2(D)$  by  $\text{N}(m, C)$  where  $C: L^2(D) \rightarrow L^2(D)$  denotes the associated covariance operator defined by  $Cv(t) = \int_D c(s, t)v(s) ds$ . Given the eigenpairs  $(\lambda_i, \phi_i)$  of  $C$ , we obtain the Karhunen–Loève expansion for the level set function  $g$ ,

$$g = g(X) = m + \sum_{i=1}^{\infty} \phi_i X_i, \quad X_i \sim \text{N}(0, \lambda_i), \quad (5.4)$$

where the  $X_i$  are stochastically independent and the random sequence  $X := (X_i)_{i \in \mathbb{N}}$  belongs almost surely to  $\ell^2$ . Thus, inferring  $g$  coincides with inferring the coefficients  $X \in \ell^2$  in (5.4), based on the noisy data  $y = O \circ G \circ \mathcal{L}(g(X)) + \eta$ . If  $m \equiv 0$ , then given the invariance of the level set map  $\mathcal{L}$  under radial projection, it follows that  $\mathcal{L}(g(\alpha x)) = \mathcal{L}(g(x))$  for any sequence  $x = (x_i)_{i \in \mathbb{N}} \in \ell^2$  of coefficients in (5.4) and any  $\alpha > 0$ . Hence, the inverse problem can be formulated on the unit sphere  $\mathbb{S} \subset \ell^2$ . The corresponding prior is then an ACG measure  $\mu_0 = \text{ACG}(\Lambda)$  where  $\Lambda = \text{diag}(\lambda_i : i \in \mathbb{N})$ . This prior is the push-forward of  $\text{N}(0, \Lambda)$  on  $\ell^2$  under the radial projection  $\Pi^{\mathbb{S}}$ .

**Remark 5.1** (Boundedness of  $\bar{\Phi}$ ). Given that  $\eta \sim \text{N}(0, \Sigma)$ , the negative log likelihood  $\bar{\Phi}$  for Bayesian level set inversion on  $\mathbb{S}$  takes the form

$$\bar{\Phi}(\bar{x}) := \frac{1}{2} \left\| \Sigma^{-1/2} (y - O \circ G \circ \mathcal{L}(g(\bar{x}))) \right\|^2.$$

Since the range of  $\mathcal{L}$  is bounded in  $L^\infty(D)$ , i.e.  $\|\mathcal{L}(g)\|_{L^\infty(D)} \leq \max_i |u_i|$ , and since  $G$  and  $O$  are locally Lipschitz continuous and bounded respectively, we obtain that also  $\bar{\Phi}$  is bounded on  $\mathbb{S}$ . Thus, the setting of Bayesian level set inversion satisfies the assumptions of Theorem 4.7. In particular, for finite-dimensional approximations of the Bayesian level set inversion problem that are obtained by truncating the expansion (5.4) after  $d$  terms, Algorithms 4, 5 and 7 yield uniformly ergodic Markov chains on  $\mathbb{S}^{d-1}$  targeting the corresponding posterior  $\mu^{(d)}$ .

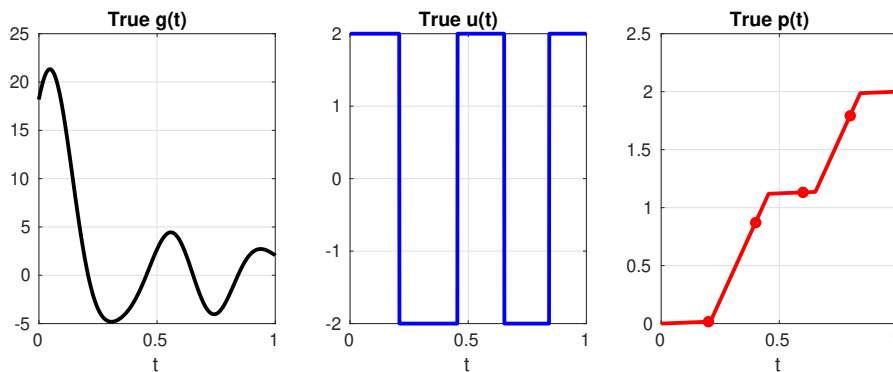


**Figure 5.1.:** True  $g^\dagger$ ,  $u^\dagger$ ,  $p^\dagger$ , and true observations  $o^\dagger = (p^\dagger(0.2), \dots, p^\dagger(0.8))^\top$ .

## 5.2. Numerical Bayesian binary classification for elliptic PDE

We consider the elliptic problem (5.1) on  $D = [0, 1]$  with Dirichlet data  $p(0) = 0$  and  $p(1) = 2$ . For  $u$  we assume a decomposition of  $D$  into two subregions  $D_1, D_2$  with corresponding values  $u_1 = -2$  and  $u_2 = 2$ . Thus, our model for  $u$  given a level set function  $g$  is

$$u(t) = \mathcal{L}(g)(t) = -2 + 4 \cdot \mathbf{1}_{[0, \infty)}(g(t)), \quad t \in D, \quad (5.5)$$

using a threshold  $\gamma_1 = 0$ . For  $g$  we assume a mean zero Gaussian process with covariance function

$$c(s, t) = \left(1 + \sqrt{3} \frac{|t - s|}{0.1}\right) \exp\left(-\sqrt{3} \frac{|t - s|}{0.1}\right), \quad (5.6)$$

i.e. a Whittle–Matérn covariance with variance  $\sigma^2 = 1$ , correlation length  $\rho = 0.1$  and smoothness  $\nu = 1.5$ . We compute the corresponding Karhunen–Loève expansion (5.4) and truncate it after  $d$  terms, for numerical simulations. We then infer the  $d$  coefficients  $x_1, \dots, x_d$  in the representation (5.4) of  $g$  given noisy observations of  $p(0.2)$ ,  $p(0.4)$ ,  $p(0.6)$ , and  $p(0.8)$ . The assumed noise model is  $\eta \sim \mathcal{N}(0, \Sigma)$  where  $\Sigma = \text{diag}(\sigma_1^2, \dots, \sigma_4^2)$  and  $\sigma_i^2 = p^\dagger(0.2j)/10$  where  $p^\dagger$  denotes the “true” solution resulting from the “true” coefficient vector  $x^\dagger = (1, 2, 3, 4, 5, 1, 1, 1, 0, \dots, 0)$  in the Karhunen–Loève expansion (5.4) of  $g^\dagger$ . For an illustration of  $g^\dagger$ ,  $u^\dagger$  and  $p^\dagger$ , see Figure 5.1.

Given  $\eta \sim \mathcal{N}(0, \Sigma)$  the negative log-likelihood for observed data  $y \in \mathbb{R}^4$  is then

$$\Phi(x) := \frac{1}{2} \sum_{j=1}^4 \sigma_j^{-2} |y_j - F_j(x)|^2, \quad x \in \mathbb{R}^d,$$

where  $F_j$  denotes the forward mapping  $x = (x_i)_{i=1}^d \mapsto g \mapsto u \mapsto p \mapsto p(0.2j)$ . As described in the previous subsection, we have  $F_j(\alpha x) = F_j(x)$  for every  $x \in \mathbb{R}^d$  and  $\alpha > 0$ . Thus,  $\Phi$  is invariant under the radial projection map  $\Pi^{\mathbb{S}}$ , i.e.  $\Phi \circ \Pi^{\mathbb{S}} = \Phi$ , and we can consider Bayesian level set inversion on the sphere  $\mathbb{S}^{d-1}$  with corresponding prior

$$\mu_0 = \text{ACG}(\Lambda_d), \quad \Lambda_d = \text{diag}(\lambda_1, \dots, \lambda_d).$$

The posterior  $\mu$  then takes the form (4.1) with  $\bar{\Phi}(\bar{x}) = \Phi(\bar{x})$ . We illustrate the prior, the likelihood and the resulting posterior for  $d = 3$  dimensions in Figure 5.2.

**Remark 5.2.** The eigenpairs  $(\lambda_j, \phi_j)$  of the covariance operator  $C$  associated to  $c$  in (5.6) are computed numerically via a discretisation of  $D$  and  $C$  using a grid size of length  $\delta t = 10^{-3}$ . The elliptic problem (5.1) is solved numerically using the same discretisation. Note that the solution  $p$  of (5.1) on  $D = [0, 1]$  is given by  $G(u)(t) = p(t) = 2S_t(e^{-u})/S_1(e^{-u})$  with  $S_t(f) = \int_0^t f(s)ds$ . We evaluate  $S_t$  using the trapezoidal rule on the given grid.

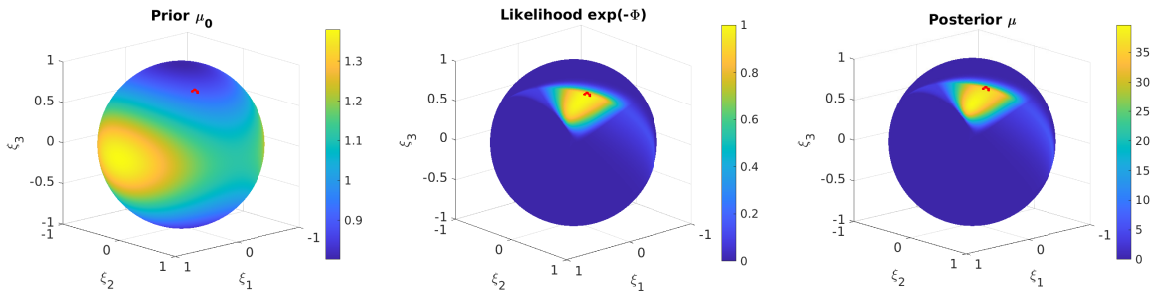


**Figure 5.2.:** Prior, likelihood and posterior for  $m = 3$  dimensions; the red spot indicates the (projected) truth  $\bar{x}^\dagger$ .

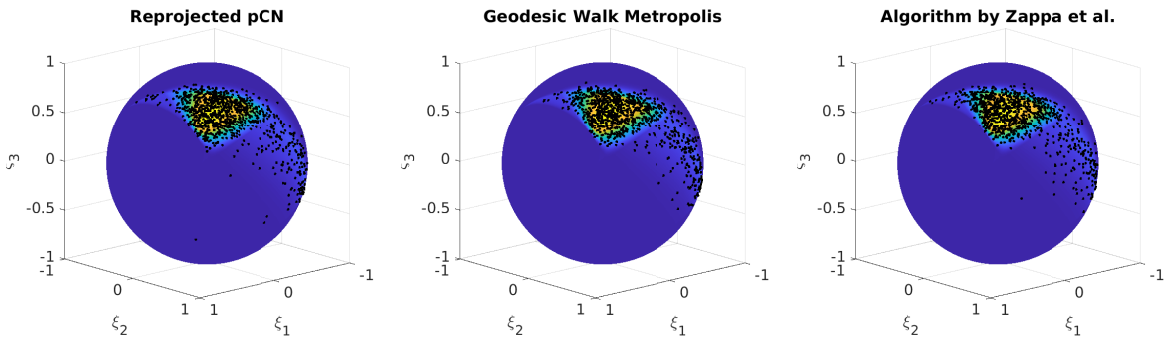


**Figure 5.3.:** Thinned realisations  $\bar{x}_{100k}$ ,  $k = 1, \dots, 100$  of the Markov chains generated by [Algorithm 4](#) (left), [Algorithm 6](#) (middle) and [Algorithm 7](#) (right) for  $d = 3$ , subsampled every 100 steps.

**MCMC on the sphere.** We now apply the four MCMC algorithms described in [Section 4](#) in order to sample approximately from the posterior  $\mu$  in various dimensions  $d$ . In particular, we aim to compute the posterior expectation of the following quantity of interest:

$$q(\bar{x}) = \left( \int_D \exp(-u(t, \bar{x})) dt \right)^{-1}$$

where  $u(\cdot, \bar{x}) = \mathcal{L}(g(\bar{x}))$ . We may interpret  $q(\bar{x})$  as the effective homogenised permeability field over the one-dimensional domain  $D$ ; see e.g. ([Alexanderian, 2015](#), Section 2).

First, we show in [Figure 5.3](#) the thinned realisations  $\bar{x}_{100k}$ ,  $k = 1, \dots, 100$  of the Markov chains generated by the reprojected pCN-MH algorithm, the geodesic random walk-MH algorithm based on ([Mangoubi and Smith, 2018](#)), and the MH algorithm of ([Zappa et al., 2018](#)) for  $d = 3$ , subsampled every 100 steps.

All three MH algorithms were tuned to an average acceptance rate of roughly 23%. We ran the algorithms for another  $10^6$  iterations after a burn-in period of  $5 \cdot 10^4$  iterations. All three runs yielded similar estimates for the posterior expectation of  $q$ . We provide the corresponding estimate plus/minus the half-length of a 95% confidence interval based on asymptotic variance estimates via empirical autocorrelation functions  $(q(\bar{x}_k))_k$ :

$$\begin{aligned} \text{reprojected pCN-MH} &: 0.420 \pm 1.299 \cdot 10^{-3} \\ \text{Geodesic random walk-MH} &: 0.419 \pm 1.271 \cdot 10^{-3} \\ \text{MH by Zappa et al.} &: 0.420 \pm 1.478 \cdot 10^{-3}. \end{aligned}$$

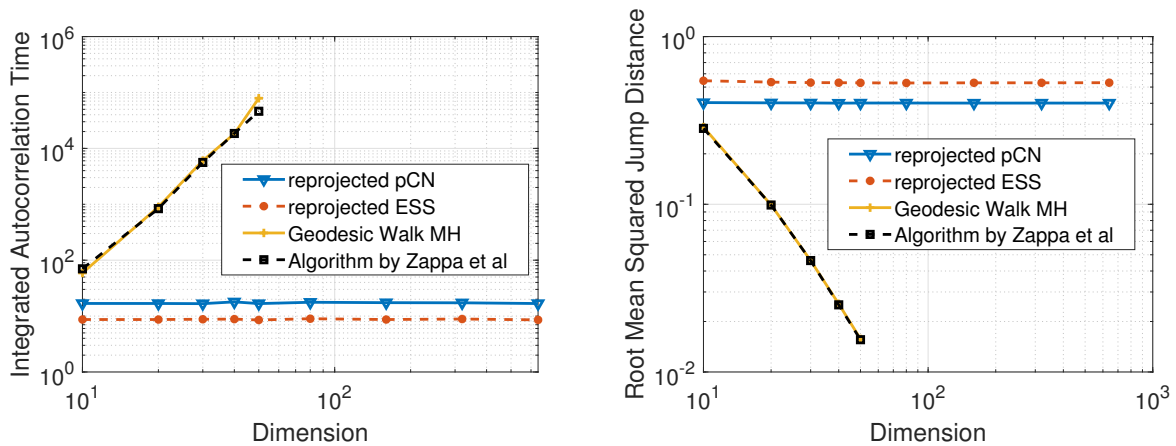


**Figure 5.4.:** Estimated integrated autocorrelation time (left) and root mean squared jump distance (right) for Algorithm 4, Algorithm 5, Algorithm 6, and Algorithm 7.

All three estimates come with similar accuracy. In terms of root mean squared jump distance with respect to the Riemannian metric on the sphere

$$\text{RMSJD} := \sqrt{\frac{1}{n-1} \sum_{k=1}^{n-1} d_{\mathbb{S}}^2(\bar{x}_k, \bar{x}_{k+1})}$$

in dimension  $d = 3$ , the three MH algorithms yielded similar estimates for the posterior expectation of  $q$ :

$$\begin{aligned} \text{reprojected pCN-MH} &: 0.202 \\ \text{Geodesic random walk-MH} &: 0.234 \\ \text{MH by Zappa et al.} &: 0.185. \end{aligned}$$

Next, we test all four algorithms, including now the reprojected ESS algorithm for increasing dimensions  $d = 10, 20, 40, 80, 160, 320, 640$ . In particular, we display the following quantities:

- (i) the estimated integrated autocorrelation time of the (approximately stationary) time series  $(q(\bar{x}_k))_k$  as a measure for the MCMC error for computing the posterior expectation of  $q$ ;
- (ii) the root mean squared jump distance as a measure of how well the Markov chain explores the sphere.

We display the results in Figure 5.4. An important observation from Figure 5.4 is that the two reprojected MCMC methods show dimension-independent efficiency in terms of integrated autocorrelation time and root mean squared jump distance. In contrast, the two MH algorithms relying on the surface measure as reference measure — namely, the geodesic random walk-MH algorithm based on (Mangoubi and Smith, 2018) and the MH algorithm of (Zappa et al., 2018) — show a clear decrease in efficiency as the dimension  $d$  of the state space increases. While it seems that the ESS algorithm yields a higher efficiency, the higher efficiency comes at an increased cost: on average, the ESS algorithm required  $\approx 3.8$  tries until it hit the level set. Thus, the computational cost of the ESS algorithm was roughly four times higher than the computational cost of the pCN algorithm.

## 6. Closing remarks

In this paper, we proposed efficient MCMC algorithms for sampling target measures on high-dimensional spheres that are absolutely continuous with respect to an ACG prior. Our algorithms exploit the structure of the ACG prior by lifting the sampling problem on the sphere to a sampling problem in the ambient Hilbert space. This allows us to apply existing MCMC algorithms on linear spaces — such as the pCN-MH algorithm — for which there are theoretical results concerning dimension-independent efficiency.

Using the methodology of push-forward Markov kernels, we then obtained transition kernels on the sphere that inherit many properties of the transition kernels in the ambient Hilbert space, e.g. reversibility with respect to the desired target measure. Under fairly mild conditions, we showed the uniform ergodicity of Markov chains generated by our algorithms, and provided theoretical arguments for the dimension independence of their spectral gaps. A complete proof of dimension independence was out of the scope of this paper.

Using binary classification as a test problem, we compared the performance of our methods to that of MH algorithms based on the geodesic random walk proposal of [Mangoubi and Smith \(2018\)](#) and the approach of [Zappa et al. \(2018\)](#). Our results illustrated the robustness of our algorithms as the dimension of the state space increased. In comparison, the statistical efficiency of the two other existing algorithms decreased as the dimension of the state space increased.

Based on our work, several interesting questions for future research remain. For instance, the possibility of weakening the condition of Lipschitz continuity stated in [Theorem 4.9](#), which would yield a theoretical proof of dimension independence of the reprojected pCN-MH. Similarly, a theoretical analysis of the dimension independence of the (reprojected) ESS transition kernel remains an open issue. Here Markov chain comparison techniques — as have been developed by, for example, [Peskun \(1973\)](#), [Andrieu and Vihola \(2016\)](#), and [Rudolf and Sprungk \(2018\)](#) — may be useful for establishing the inheritance of a spectral gap from the pCN-MH transition kernel to the ESS transition kernel. Additionally, it seems promising to modify our algorithms so that they can be applied to sample from target measures with respect to other common priors such as Bingham distributions, by using the acceptance-rejection approach in ([Kent et al., 2018](#)), for example.

## Acknowledgements

The research of HCL has been partially funded by the Deutsche Forschungsgemeinschaft (DFG) — Project-ID [318763901](#) — SFB1294. BS has been supported by the DFG project [389483880](#). DR gratefully acknowledges partial support of the [Felix Bernstein Institute for Mathematical Statistics in the Biosciences](#) and the DFG within project [432680300](#) — SFB 1456. TJS has been partially supported by the Freie Universität Berlin and the Zuse Institute Berlin within the Excellence Initiative of the DFG, and by DFG projects [390685689](#) and [415980428](#). The authors wish to thank S. Huckemann and M. Habeck for helpful discussions.

## References

- A. Alexanderian. Expository paper: A primer on homogenization of elliptic PDEs with stationary and ergodic random coefficient functions. *Rocky Mountain J. Math.*, 45(3):703–735, 2015. [doi:10.1216/RMJ-2015-45-3-703](#).
- C. Andrieu and M. Vihola. Establishing some order amongst exact approximations of MCMCs. *Ann. Appl. Probab.*, 26(5):2661–2696, 2016. [doi:10.1214/15-AAP1158](#).

- S. Asmussen and P. W. Glynn. A new proof of convergence of MCMC via the ergodic theorem. *Statist. Probab. Lett.*, 81(10):1482–1485, 2011. doi:10.1016/j.spl.2011.05.004.
- A. Beskos, G. Roberts, A. M. Stuart, and J. Voss. MCMC methods for diffusion bridges. *Stoch. Dyn.*, 8(3):319–350, 2008. doi:10.1142/S0219493708002378.
- A. Beskos, M. Girolami, S. Lan, P. E. Farrell, and A. M. Stuart. Geometric MCMC for infinite-dimensional inverse problems. *J. Comput. Phys.*, 335:327–351, 2017. doi:10.1016/j.jcp.2016.12.041.
- V. I. Bogachev. *Gaussian Measures*, volume 62 of *Mathematical Surveys and Monographs*. American Mathematical Society, Providence, RI, 1998. doi:10.1090/surv/062.
- A. Bonito, A. Cohen, R. DeVore, G. Petrova, and G. Welper. Diffusion coefficients estimation for elliptic partial differential equations. *SIAM J. Math. Anal.*, 49(2):1570–1592, 2017. doi:10.1137/16M1094476.
- M. Brubaker, M. Salzmann, and R. Urtasun. A family of MCMC methods on implicitly defined manifolds. In N. D. Lawrence and M. Girolami, editors, *Proceedings of the Fifteenth International Conference on Artificial Intelligence and Statistics*, volume 22 of *Proceedings of Machine Learning Research*, pages 161–172, La Palma, Canary Islands, 21–23 Apr 2012. PMLR. URL <http://proceedings.mlr.press/v22/brubaker12/brubaker12.pdf>.
- S. Byrne and M. Girolami. Geodesic Monte Carlo on embedded manifolds. *Scand. J. Stat.*, 40(4):825–845, 2013. doi:10.1111/sjos.12036.
- V. Chen, M. M. Dunlop, O. Papaspiliopoulos, and A. M. Stuart. Dimension-robust MCMC in Bayesian inverse problems, 2018. arXiv:1803.03344.
- Y. Chikuse. *Statistics on Special Manifolds*, volume 174 of *Lecture Notes in Statistics*. Springer, New York, NY, 2003. doi:10.1007/978-0-387-21540-2.
- S. L. Cotter, G. O. Roberts, A. M. Stuart, and D. White. MCMC methods for functions: modifying old algorithms to make them faster. *Statist. Sci.*, 28(3):424–446, 2013. doi:10.1214/13-STS421.
- P. Diaconis, S. Holmes, and M. Shahshahani. Sampling from a manifold. In *Advances in modern statistical theory and applications. A Festschrift in honor of Morris L. Eaton*, pages 102–125. Institute of Mathematical Statistics, Beachwood, OH, 2013. doi:10.1214/12-IMSCOLL1006.
- R. Douc, E. Moulines, P. Priouret, and P. Soulier. *Markov Chains*. Springer Series in Operations Research and Financial Engineering. Springer, Cham, 2018. doi:10.1007/978-3-319-97704-1.
- I. L. Dryden. Statistical analysis on high-dimensional spheres and shape spaces. *Ann. Statist.*, 33(4):1643–1665, 2005. doi:10.1214/009053605000000264.
- M. M. Dunlop, M. A. Iglesias, and A. M. Stuart. Hierarchical Bayesian level set inversion. *Statist. Comput.*, 27:1555–1584, 2017. doi:10.1007/s11222-016-9704-8.
- J. Fan, B. Jiang, and Q. Sun. Hoeffding’s inequality for general Markov chains and its applications to statistical learning. *J. Mach. Learn. Res.*, 22(139):1–35, 2021. URL <https://www.jmlr.org/papers/volume22/19-479/19-479.pdf>.
- J. Franke, C. Redenbach, and N. Zhang. On a mixture model for directional data on the sphere. *Scand. J. Stat.*, 43(1):139–155, 2016. doi:10.1111/sjos.12169.
- J. Glover and J. Mitro. Symmetries and functions of Markov processes. *Ann. Probab.*, 18(2):655–668, 1990. doi:10.1214/aop/1176990851.
- M. Hairer, A. M. Stuart, and S. J. Vollmer. Spectral gaps for a Metropolis–Hastings algorithm in infinite dimensions. *Ann. Appl. Probab.*, 24(6):2455–2490, 2014. doi:10.1214/13-AAP982.
- A. Holbrook, S. Lan, J. Streets, and B. Shahbaba. Nonparametric Fisher geometry with application to density estimation. In J. Peters and D. Sontag, editors, *Proceedings of the 36th Conference on Uncertainty in Artificial Intelligence (UAI)*, volume 124 of *Proceedings of Machine Learning Research*, pages 101–110. PMLR, 03–06 Aug 2020. URL <http://proceedings.mlr.press/v124/holbrook20a/holbrook20a.pdf>.

- M. A. Iglesias, Y. Lu, and A. M. Stuart. A Bayesian level set method for geometric inverse problems. *Interfaces Free Bound.*, 18(2):181–217, 2016. doi:10.4171/IFB/362.
- A. S. Kechris. *Classical Descriptive Set Theory*, volume 156 of *Graduate Texts in Mathematics*. Springer-Verlag, New York, 1995. doi:10.1007/978-1-4612-4190-4.
- J. T. Kent, A. M. Ganeiber, and K. V. Mardia. A new unified approach for the simulation of a wide class of directional distributions. *J. Comput. Graph. Stat.*, 27(2):291–301, 2018. doi:10.1080/10618600.2017.1390468.
- S. Lan, B. Zhou, and B. Shahbaba. Spherical Hamiltonian Monte Carlo for constrained target distributions. In E. P. Xing and T. Jebara, editors, *Proceedings of the 31st International Conference on Machine Learning*, volume 32 of *Proceedings of Machine Learning Research*, pages 629–637, Beijing, China, 22–24 Jun 2014. PMLR. URL <http://proceedings.mlr.press/v32/lan14.pdf>.
- K. Łatuszyński and W. Niemirow. Rigorous confidence bounds for MCMC under a geometric drift condition. *J. Complexity*, 27(1):23–38, 2011. doi:10.1016/j.jco.2010.07.003.
- K. Łatuszyński and D. Rudolf. Convergence of hybrid slice sampling via spectral gap, 2014. arXiv:1409.2709.
- K. Łatuszyński, B. Miasojedow, and W. Niemirow. Nonasymptotic bounds on the estimation error of MCMC algorithms. *Bernoulli*, 19(5A):2033–2066, 2013. doi:10.3150/12-BEJ442.
- C. Ley and T. Verdebout. *Modern Directional Statistics*. Chapman & Hall/CRC Interdisciplinary Statistics Series. CRC Press, Boca Raton, FL, 2017. doi:10.1201/9781315119472.
- Y. Li and S. G. Walker. A latent slice sampling algorithm, 2020. arXiv:2010.08509.
- O. Mangoubi and A. Smith. Rapid mixing of geodesic walks on manifolds with positive curvature. *Ann. Appl. Probab.*, 28(4):2501–2543, 2018. doi:10.1214/17-AAP1365.
- K. V. Mardia and P. E. Jupp. *Directional Statistics*. Wiley Series in Probability and Statistics. John Wiley & Sons, Ltd., Chichester, 2000. doi:10.1002/9780470316979. Revised reprint of *Statistics of Directional Data* by K. V. Mardia.
- S. Meyn and R. L. Tweedie. *Markov Chains and Stochastic Stability*. Cambridge University Press, Cambridge, second edition, 2009. doi:10.1017/CBO9780511626630.
- I. Murray, R. Adams, and D. MacKay. Elliptical slice sampling. In Y. W. Teh and M. Titterton, editors, *Proceedings of the Thirteenth International Conference on Artificial Intelligence and Statistics*, volume 9 of *Proceedings of Machine Learning Research*, pages 541–548. 2010. URL <https://proceedings.mlr.press/v9/murray10a.html>.
- V. Natarovskii. *Geometric Convergence of Slice Sampling*. Dissertation Dr.rer.nat., Georg-August-Universität Göttingen, 2021. URL <http://hdl.handle.net/21.11130/00-1735-0000-0008-5948-4>.
- V. Natarovskii, D. Rudolf, and B. Sprungk. Geometric convergence of elliptical slice sampling. In M. Meila and T. Zhang, editors, *Proceedings of the 38th International Conference on Machine Learning*, volume 139 of *Proceedings of Machine Learning Research*, pages 7969–7978, 2021a. URL <http://proceedings.mlr.press/v139/natarovskii21a/natarovskii21a.pdf>.
- V. Natarovskii, D. Rudolf, and B. Sprungk. Quantitative spectral gap estimate and Wasserstein contraction of simple slice sampling. *Ann. Appl. Probab.*, 31(2):806–825, 2021b. doi:10.1214/20-AAP1605.
- R. M. Neal. Regression and classification using Gaussian process priors. (With discussion). In J. M. Bernardo, J. O. Berger, A. P. Dawid, and A. F. M. Smith, editors, *Bayesian Statistics 6. Proceedings of the Sixth Valencia International Meeting, 1998*, pages 475–501. Clarendon Press, Oxford, 1999.
- R. M. Neal. Slice sampling. *Ann. Statist.*, 31(3):705–767, 2003. doi:10.1214/aos/1056562461.
- E. Novak and D. Rudolf. Computation of expectations by Markov chain Monte Carlo methods. In *Extraction of Quantifiable Information from Complex Systems*, Lecture Notes in



- Computational Science and Engineering, pages 397–411. Springer, 2014. doi:10.1007/978-3-319-08159-5\_20.
- D. Paulin. Concentration inequalities for Markov chains by Marton couplings and spectral methods. *Electron. J. Probab.*, 20:1–32, 2015. doi:10.1214/EJP.v20-4039.
- P. H. Peskun. Optimum Monte-Carlo sampling using Markov chains. *Biometrika*, 60(3):607–612, 12 1973. doi:10.1093/biomet/60.3.607.
- M. Rosenblatt. Functions of Markov processes. *Z. Wahrscheinlichkeitstheor. Verw. Geb.*, 5: 232–243, 1966. doi:10.1007/BF00533060.
- D. Rudolf. Explicit error bounds for Markov chain Monte Carlo. *Dissertationes Math.*, 485: 1–93, 2012. doi:10.4064/dm485-0-1.
- D. Rudolf and N. Schweizer. Error bounds of MCMC for functions with unbounded stationary variance. *Statist. Probab. Lett.*, 99:6–12, 2015. doi:10.1016/j.spl.2014.07.035.
- D. Rudolf and B. Sprungk. On a generalization of the preconditioned Crank–Nicolson Metropolis Algorithm. *Found. Comput. Math.*, 18:309–343, 2018. doi:10.1007/s10208-016-9340-x.
- D. Rudolf and B. Sprungk. Robust random walk-like Metropolis–Hastings algorithms for concentrating posteriors, 2022. arXiv:2202.12127.
- A. Srivastava and I. H. Jermyn. Looking for shapes in two-dimensional cluttered point clouds. *IEEE Trans. Pattern Anal. Machine Intell.*, 31(9):1616–1629, 2009. doi:10.1109/TPAMI.2008.223.
- K. Tabelow, H. U. Voss, and J. Polzehl. Modeling the orientation distribution function by mixtures of angular central Gaussian distributions. *J. Neurosci. Meth.*, 203(1):200–211, 2012. doi:10.1016/j.jneumeth.2011.09.001.
- L. Tierney. A note on Metropolis–Hastings kernels for general state spaces. *Ann. Appl. Probab.*, 8(1):1–9, 1998. doi:10.1214/aoap/1027961031.
- D. E. Tyler. Statistical analysis for the angular central Gaussian distribution on the sphere. *Biometrika*, 74(3):579–589, 1987. doi:10.1093/biomet/74.3.579.
- F. Wang and A. E. Gelfand. Directional data analysis under the general projected normal distribution. *Stat. Methodol.*, 10(1):113–127, 2013. doi:10.1016/j.stamet.2012.07.005.
- G. S. Watson. *Statistics on Spheres*, volume 6 of *University of Arkansas Lecture Notes in the Mathematical Sciences*. John Wiley & Sons, Inc., New York, 1983.
- E. Zappa, M. Holmes-Cerfon, and J. Goodman. Monte Carlo on manifolds: Sampling densities and integrating functions. *Commun. Pure Appl. Anal.*, 71(12):2609–2647, 2018. doi:10.1002/cpa.21783.

## A. Topology of the Hilbert sphere

**Lemma A.1.** *The topology on  $\mathbb{S}$  generated by  $d_{\mathbb{S}}$  coincides with the relative topology on  $\mathbb{S}$  generated by the norm  $\|\cdot\|$  of  $\mathbb{H}$ .*

**Proof.** This is a consequence of the Lipschitz equivalence of the metrics (2.7). ■

**Corollary A.2.** *Let  $C_E := \{\alpha e \mid \alpha > 0, e \in E\} \subseteq \mathbb{H}$  denote the cone spanned by a subset  $E \subseteq \mathbb{S}$ . The set  $E$  is open in  $(\mathbb{S}, d_{\mathbb{S}})$  if and only if  $C_E$  is open in  $(\mathbb{H}, \|\cdot\|)$ .*

**Proof.** Suppose that  $C_E$  is open in  $\mathbb{H}$ . Then  $E = C_E \cap \mathbb{S}$  is, by Lemma A.1, open in  $(\mathbb{S}, d_{\mathbb{S}})$ .

Let  $\Pi^{\mathbb{S}}|_{\mathbb{H} \setminus \{0\}}$  be the restriction of the radial projection  $\Pi^{\mathbb{S}}$  defined in (2.8) to  $\mathbb{H} \setminus \{0\}$ . For  $E$  in  $(\mathbb{S}, d_{\mathbb{S}})$ ,  $(\Pi^{\mathbb{S}}|_{\mathbb{H} \setminus \{0\}})^{-1}(E) = C_E$ . Equip  $\mathbb{H} \setminus \{0\}$  with the subspace topology. Then  $\Pi^{\mathbb{S}}|_{\mathbb{H} \setminus \{0\}}$  is continuous, and if  $E$  is open, then  $C_E$  is open in  $(\mathbb{H} \setminus \{0\}, \|\cdot\|)$ , and hence in  $(\mathbb{H}, \|\cdot\|)$ . ■

## B. Counterexample for the Markovianity of $T(X_k)$

Let  $\mathbb{H} = \mathbb{R}^d$ ,  $d > 1$ , and  $\Pi^{\mathbb{S}}$  be the radial projection onto the unit sphere in  $\mathbb{H}$  as in (2.8), where we have fixed  $\bar{z} = e_d = (0, \dots, 0, 1)^\top$ . Moreover, let  $(X_n)_{n \in \mathbb{N}}$  denote a Markov chain on  $\mathbb{H}$  with transition kernel  $K$ .

If  $(\Pi^{\mathbb{S}}(X_n))_{n \in \mathbb{N}}$  were again a Markov chain, then we would have for the ‘‘upper half’’ of the sphere  $H_d := \{x = (x_1, \dots, x_d)^\top \in \mathbb{S} \mid x_d \geq 0\}$  that

$$\mathbb{P}(\Pi^{\mathbb{S}}(X_2) \in H_d \mid \Pi^{\mathbb{S}}(X_1) = e_d) = \mathbb{P}(\Pi^{\mathbb{S}}(X_2) \in H_d \mid \Pi^{\mathbb{S}}(X_1) = e_d, \Pi^{\mathbb{S}}(X_0) = e_d),$$

or,  $\mathbb{P}(\Pi^{\mathbb{S}}(X_{n+2}) \in H_d \mid \Pi^{\mathbb{S}}(X_{n+1}) = e_d) = \mathbb{P}(\Pi^{\mathbb{S}}(X_{n+2}) \in H_d \mid \Pi^{\mathbb{S}}(X_{n+1}) = e_d, \Pi^{\mathbb{S}}(X_n) = e_d)$  for any  $n \in \mathbb{N}$ . By definition of  $\Pi^{\mathbb{S}}$ , this is equivalent to

$$\frac{\mathbb{P}(X_{2,d} > 0, X_{1,d} > 0)}{\mathbb{P}(X_{1,d} > 0)} = \frac{\mathbb{P}(X_{2,d} > 0, X_{1,d} > 0, X_{0,d} > 0)}{\mathbb{P}(X_{1,d} > 0, X_{0,d} > 0)},$$

where  $X_n = (X_{n,1}, \dots, X_{n,d})^\top$  denotes the state vector of the Markov chain. Consider now a Markov chain  $(X_n)_{n \in \mathbb{N}}$  with initial distribution  $X_0 \sim \mathcal{N}(0, I)$  and Gaussian random walk transition kernel  $K(x, \cdot) = \mathcal{N}(x, s^2 I)$  for a fixed step size  $s > 0$ . Then each component of the states is a Markov chain independent of the other components. Hence,

$$\frac{\mathbb{P}(X_{2,d} > 0, X_{1,d} > 0)}{\mathbb{P}(X_{1,d} > 0)} = \frac{\mathbb{P}(W_0 + sW_1 + sW_2 > 0, W_0 + sW_1 > 0)}{\mathbb{P}(W_0 + sW_1 > 0)}$$

for  $W_0, W_1, W_2 \stackrel{\text{i.i.d.}}{\sim} \mathcal{N}(0, 1)$  and, analogously,

$$\frac{\mathbb{P}(X_{2,d} > 0, X_{1,d}, X_{0,d} > 0)}{\mathbb{P}(X_{1,d} > 0, X_{0,d} > 0)} = \frac{\mathbb{P}(W_0 + sW_1 + sW_2 > 0, W_0 + sW_1 > 0, W_0 > 0)}{\mathbb{P}(W_0 + sW_1 > 0, W_0 > 0)}.$$

The expressions for these probabilities are difficult to evaluate exactly. Therefore, we perform a Monte Carlo integration using  $10^8$  samples and obtain the following estimates for  $s = 1$ :

$$\begin{aligned} \frac{\mathbb{P}(W_0 + sW_1 + sW_2 > 0, W_0 + sW_1 > 0)}{\mathbb{P}(W_0 + sW_1 > 0)} &\approx 0.8041, \\ \frac{\mathbb{P}(W_0 + sW_1 + sW_2 > 0, W_0 + sW_1 > 0, W_0 > 0)}{\mathbb{P}(W_0 + sW_1 > 0, W_0 > 0)} &\approx 0.8333. \end{aligned}$$

We now show that the above observation is not restricted to the random walk transition kernel. Consider a stationary Markov chain generated by the pCN proposal kernel  $Q(x, \cdot) = \mathcal{N}(\sqrt{1-s^2}x, s^2 I)$  and initial distribution  $X_0 \sim \mathcal{N}(0, I)$ . We again obtain independent scalar Markov chains in each component:

$$\frac{\mathbb{P}(X_{2,d} > 0, X_{1,d} > 0)}{\mathbb{P}(X_{1,d} > 0)} = \frac{\mathbb{P}((1-s^2)W_0 + s\sqrt{1-s^2}W_1 + sW_2 > 0, \sqrt{1-s^2}W_0 + sW_1 > 0)}{\mathbb{P}(\sqrt{1-s^2}W_0 + sW_1 > 0)}$$

as well as

$$\begin{aligned} \frac{\mathbb{P}(X_{2,d} > 0, X_{1,d}, X_{0,d} > 0)}{\mathbb{P}(X_{1,d} > 0, X_{0,d} > 0)} &= \frac{\mathbb{P}((1-s^2)W_0 + s\sqrt{1-s^2}W_1 + sW_2 > 0, \sqrt{1-s^2}W_0 + sW_1 > 0, W_0 > 0)}{\mathbb{P}(\sqrt{1-s^2}W_0 + sW_1 > 0, W_0 > 0)}, \end{aligned}$$

where  $W_0, W_1, W_2 \stackrel{\text{iid}}{\sim} N(0, 1)$ . Monte Carlo integration with the stationary pCN-generated Markov chain,  $s = 0.5$ , and  $10^8$  samples yields

$$\frac{\mathbb{P}(X_{2,d} > 0, X_{1,d} > 0)}{\mathbb{P}(X_{1,d} > 0)} \approx 0.8333, \quad \frac{\mathbb{P}(X_{2,d} > 0, X_{1,d}, X_{0,d} > 0)}{\mathbb{P}(X_{1,d} > 0, X_{0,d} > 0)} \approx 0.8620.$$

Thus, these Markov chains serve as counterexamples to the claim that  $(\Pi^{\mathbb{S}}(X_n))_{n \in \mathbb{N}}$  is again a Markov chain.